

AN ABSTRACT OF THE THESIS OF

Tomás Rodrigo Fonseca for the degree of Master of Science  
in Oceanography presented on 20 August 1981

Title: ON PHYSICAL CHARACTERISTICS OF UPWELLING EVENTS OFF OREGON  
AND PERU

Abstract approved: **Redacted for privacy**  
Dr. Robert L. Smith

A description of the physical oceanographic conditions during coastal upwelling events (periods of intense upwelling favorable winds) observed off Oregon (near 45° N) and Peru (near 15° S) is made using data from a similar number of current meter moorings located at mid-shelf. Wind measurements from anemometers mounted on buoys are used to determine the locally forced response in the currents. Sea level observations from coastal tide gauges are also used to study the dynamics of upwelling events.

Since most of the past observational research on upwelling is based on the analysis of patterns on the entire records of data of several month duration, not much information on the specific, short term upwelling events has been published. In this thesis, the response of the coastal ocean to individual wind events is compared to that reported in the literature, based on statistical analysis of entire records.

Three periods of upwelling events were selected in both areas. In addition, a short period of poleward wind over the Oregon shelf was used to study a downwelling event. There was a clear response of the coastal waters, off Oregon and Peru, to periods of upwelling events. At the surface, both temperature and velocity fields intensify during events; the peak values reached by them are one standard deviation higher than the

complete record mean. The time lag between the maximum wind and the maximum offshore flow is approximately zero off Oregon. On the other hand off Peru, the maximum offshore flow tended to precede the maximum wind by less than a day. In both locations there is a surface equatorward flow which reached a maximum value in less than a day after the maximum wind. There is a poleward undercurrent off both Oregon and Peru. In Oregon it disappears during events, and appears again during relaxation of the event; usually three or four days after the maximum wind. On the contrary, off Peru the undercurrent was present all the time.

The dynamics of upwelling events was studied comparing the magnitudes of the terms involving horizontal velocities in the linear momentum equations. The results show that the momentum balance during events is analogous to the mean momentum balance during the upwelling season: the alongshore velocity is in geostrophic balance, the offshore transport in the surface agrees well with the calculated Ekman transport, and the onshore transport in the interior is about twice as large as the offshore wind-driven transport. The lack of two dimensional mass balance, i.e., the failure for the offshore flow in the surface layer to be balanced by the deeper onshore flow, during upwelling events as well as in the mean, point to the importance of alongshore variations. In other words coastal upwelling seems to be intrinsically three dimensional.

ON THE PHYSICAL CHARACTERISTICS OF UPWELLING  
EVENTS OFF OREGON AND PERU

by

Tomás Rodrigo Fonseca

A THESIS

submitted to

Oregon State University

in partial fulfillment of  
the requirements for the  
degree of

Master of Science

Commencement June 1982

APPROVED:

Redacted for privacy

Professor of Oceanography  
in charge of major

Redacted for privacy

Dean of the School of Oceanography

Redacted for privacy

Dean of Graduate School

Date thesis is presented 20 August 1981

Typed by Rebecca Simpkins for Tomás Rodrigo Fonseca

A MI MEJOR AMIGA,

MI ESPOSA, MARIA-ISABEL.

## ACKNOWLEDGEMENTS

I wish to give special thanks to my major professor, Dr. Robert L. Smith, for his supervision and advice.

I wish also to give thanks to Dr. David B. Enfield and Dr. Paula Kanarek, for many suggestions which helped to improve this thesis. I also give my special thanks to Dr. Steve Neshyba for his resolute and continuous support to all his former Chilean students, making possible not only our career but also enriching our lives with his constructive advising.

The data used in this thesis were collected as part of the Coastal Upwelling Ecosystem Analysis Program (CUEA) of the International Decade of Ocean Exploration, National Science Foundation. William E. Gilbert and Henry Pittock assisted in the data analysis. Dr. David Halpern of the Environmental Research Laboratory, NOAA, provided surface current measurements.

My studies at OSU were supported by the OSU-UCV agreement, and partially financed by the U. S. National Science Foundation under grant OCE-7819795.

# TABLE OF CONTENTS

<u>Chapter</u>	<u>Page</u>
I. INTRODUCTION	1
A. Literature Review	2
B. Organization of this Thesis	3
II. DATA: SOURCES AND HANDLING	6
A. CUEA Experiments	6
B. Data Processing	6
III. TIME AND DEPTH DEPENDENT CHANGES OF FLOW AND TEMPERATURE FIELDS DURING UPWELLING EVENTS	10
A. Selection of Wind Events	10
B. Mean Flow and Temperature Fields	13
C. Variability in the Flow and Temperature Fields	15
D. Flow Fields during Events	19
D. 1 Oregon	19
D. 2 Peru	24
E. Time Lags	28
F. Summary of Salient Features	37
IV. DYNAMICAL ASPECTS OF UPWELLING EVENTS	39
A. Formulation of the Momentum Equations	39
B. Review of the Mean Momentum Balance	41
C. Is the Alongshore Flow in Geostrophic Balance During Events?	45
D. Ekman Dynamics and Volume Budgets During Events?	48
E. Is the Cross-Isobath Flow in Geostrophic Balance with $P_y$ ?	50
V. DISCUSSION AND CONCLUSIONS	56
A. Response of the Flow and Temperature	56

<u>Chapter</u>	<u>Page</u>
B. Time Scale of Events	58
C. Momentum and Volume Balances	59
D. Conclusions	61
BIBLIOGRAPHY	63
APPENDIX	66
1. Notation	66



# LIST OF FIGURES

<u>Figure</u>		<u>Page</u>
1	Location of the current meter moorings (●) and pressure gauges (▲) during: (A) CUE II experiment off Oregon, July-August 1973; (B) JOINT II experiment off Peru, March-May 1977; (C) Configuration of current meter arrays and the estimated baroclinic radius of deformation, R.	7
2	Midshelf values of the wind stress components: (A) Oregon CUE II, July-August 1973; (B) Peru JOINT II, March-May 1977. Horizontal dashed lines correspond to mean values of the alongshore wind stress, and vertical bars indicate one standard deviation. Ticks on the time axis indicate 5 days periods.	11
3	Mean current profiles for the midshelf current meter array off (A) Oregon and (B) Peru (6 July to 27 August 1977 for Oregon and 22 March to 10 May 1977 for Peru).	14
4	Complete time series of velocity and temperature for CUE II from (A) surface (3.4m) and (B) near the bottom (80m). Ticks on the time axis indicate 5 days periods.	16
5	Complete time series of velocity and temperature for JOINT II from: (A) surface (4.6m) and (B) near the bottom (80m). Ticks on the time axis indicate 5 days periods.	17
6	Time-depth sections of velocity off Oregon during events (a-d), together with the wind stress and its overall mean and standard deviation. Different shaded areas indicate surface offshore-equatorward flow and deep offshore-poleward flow. Contour intervals: 5 cm/s for u and 10 cm/s for v.	20
7	Time depth sections of velocity during events off Peru (a-c). Wind stress is shown at the top together with the overall mean and the standard deviation. Shaded areas indicate surface offshore-equatorward flow. Contour intervals: 5 cm/s for u and 10 cm/s for v.	25
8	Time series of alongshore wind stress (dynes/cm <sup>2</sup> ), velocity components (cm/s), and temperature (C) for events off Oregon at 3.4m. Dashed vertical lines indicate time of maximum wind stress.	29

<u>Figure</u>		<u>Page</u>
9	Time series of alongshore wind stress (dynes/cm <sup>2</sup> ), velocity components (cm/s), and temperature (C) for events off Oregon at 80m. Dashed vertical lines indicate time of maximum wind stress.	30
10	Time series of alongshore wind stress (dynes/cm <sup>2</sup> ), velocity components (cm/s), and temperature (°C) for events off Peru at 4.6m. Dashed vertical lines indicate time of maximum wind stress.	32
11	Time series of alongshore wind stress (dynes/cm <sup>2</sup> ), velocity components (cm/s), and temperature (C) for events off Peru at 80m. Dashed lines indicate time of maximum wind stress.	33
12	Time series of terms of the horizontal momentum equations at 3.4, 40, and 60m depth off Oregon. Mean and standard deviation are also shown. Units are 10 <sup>-4</sup> cm s <sup>-2</sup> . Ticks on the time axis indicate 5 days periods.	42
13	Time series of terms of the horizontal momentum equations at 4.6, 39, and 80m depth off Peru. Mean and standard deviation are also shown. Units are 10 <sup>-4</sup> cm s <sup>-2</sup> . Ticks on the time axis indicate 5 days periods.	43
14	Cross-shelf momentum balance during events off (a) Oregon and (b) Peru. Values at 40m (39 for Peru) were used for calculations. Units are 10 <sup>-4</sup> cm s <sup>-2</sup> for fv, and cm for the adjusted sea level at newport (San Juan). The zero line correspond to the mean value for both time series ( $fv_{40}^* = fv_{40} - fv_{40}$ ).	46
15	Momentum balance in the alongshore direction off (a) Oregon and (b) Peru. Values at 40m depth were used in calculations (39m for Peru). Units are 10 <sup>-4</sup> cm s <sup>-2</sup> . The arrow on the time axis indicates the time of maximum wind stress. Pressure gradients were calculated between: Garibaldi (GA), Newport (NE) and Umpqua River (UR); off Peru were calculated between San Martin (SM) and San Juan (SJ).	51

# LIST OF TABLES

<u>Table</u>		<u>Page</u>
1	Description of the data.	8
2	Selected wind events	12
3	Time lags (hrs.) between maximum wind stress and maximum (minimum) values of variables off Oregon. Calculations were made using a 4-point parabolic fit to define time of occurrence of peaks.	35
4	Time lags (hrs.) between maximum wind stress and maximum (minimum) values of variables off Peru. Calculations were made using a 4-point parabolic fit to define time of occurrence of peaks.	36
5	Mean Ekman transport computed from the alongshore component of the wind stress during events ( $E_T$ ), measured cross-shelf transport in the surface ( $T_S$ ) and lower layer ( $T_L$ ) averaged during events. Transport is given in $10^2 \text{cm}^3/\text{cm sec}$ , and is positive toward the coast.	49

# ON THE PHYSICAL CHARACTERISTICS OF UPWELLING EVENTS OFF OREGON AND PERU

## I. INTRODUCTION

Upwelling is one of the coastal processes that has received much attention by the scientific community in the last decade. Upwelling is primarily driven by the wind stress. Along the eastern boundaries of the oceans it occurs when the alongshore equatorward component of the wind stress, acting on the sea surface, drives a component of the flow offshore. The flow that is driven offshore in the surface layer is replaced near shore by an upwelling of fluid from deeper layers. Due to the characteristic patterns of the alongshore equatorward wind, upwelling is a conspicuous feature of some coastal areas such as Oregon, Northwest Africa and Peru. The physical oceanographic conditions associated with upwelling influence important oceanic processes. For example, biological primary productivity is highly dependent on the movement of nutrient-rich water to the euphotic layer. Also, both sedimentation patterns and pollutant dispersion in coastal areas, are affected by the upwelling process (Niiler, 1975).

The Coastal Upwelling Ecosystem Analysis Program (CUEA), part of the International Decade of Ocean Exploration (1970-1980), was oriented to the study of the physical and biological aspects of the upwelling process. As part of that program major field experiments were conducted on the Oregon shelf in July-August 1973 (CUE II), and on the Peru shelf in March-April 1977 (JOINT II). Several current meter moorings were deployed in these areas for many weeks. The results of these experiments have been subjected to considerable physical oceanographic analysis

(e.g., Halpern, 1976; Huyer and Smith, 1978; Smith, 1978; Brink et al, 1980).

The upwelling favorable wind off Oregon and Peru is not constant during the upwelling season and the wind has periods of strong intensification. An increase of the equatorward alongshore wind causes more offshore transport in the surface layer, and therefore intensifies the upwelling process. Halpern (1976) and Huyer (1976) have defined periods of intense upwelling as upwelling "events".

Events tend to occur in Oregon at intervals of roughly one or two weeks (Mooers, 1976). Events also occur on the Peru shelf (Brink et al, 1978). However, since most of the past observational research on upwelling is based on a statistical approach and with analysis of patterns done on the complete series of data, not much information on the specific, short term upwelling events has been published. Therefore it is worthwhile to re-study the CUEA data, and examine if the response of the coastal ocean to individual wind events conforms to that reported in the literature for the entire records of several months duration.

#### A. Literature Review

One of the earliest studies of an upwelling event, based on direct current measurements (Halpern, 1976), describes the structure of an event observed during CUE II (Oregon). Halpern finds that the time between the onset of the upwelling favorable wind and the maximum offshore transport is of the order of one to three days. From computations of the mass balance he concludes that the observed onshore mass transport below the surface layer is nearly equal to the measured

offshore surface transport and that, in a section perpendicular to the coast, mass balance tends to be two dimensional during events in an onshore-offshore vertical plane, i.e. as having negligible gradients in velocity in the alongshore direction. In a comparison of upwelling events in Oregon and Northwest Africa, Huyer (1976) reports that the time lag between changes the circulation and the wind is less than a day. Volume budget estimations suggest that during events the mass balance tends to be two-dimensional in both areas. The question of two-dimensionality was addressed later by Allen and Kundu (1978) and Smith (1980). Using an objective definition of the coordinate axes, they find that the two-dimensionality of the mass balance is ephemeral even during events.

Even during the upwelling season, the wind is not always favorable (equatorward) for upwelling and, indeed, poleward winds do occur in the middle of the upwelling season, especially off California and Oregon. Periods of intense poleward wind are called "anti-events". The dynamics and thermodynamics of an anti-event produced by a poleward wind in midsummer along the California coast is discussed by Winant (1980). The effects of an anti-event over the Oregon shelf will also be discussed here.

The dynamics of the coastal circulation has been studied extensively. Balances of momentum have been discussed statistically and theoretically in Mooers and Allen (1973), Niiler (1975), and Allen (1980). According to earlier theoretical considerations (Ekman, 1905), the wind stress and the earth rotation cause the offshore transport in an upwelling area. This simple "Ekman dynamics" seems to hold fairly well in the upwelling season and during events (Smith, 1980).

The alongshore flow is found to be in geostrophic balance (Allen, 1980). A manifestation of this geostrophic flow is the baroclinic coastal jet, discussed theoretically by Allen (1973). In addition, perturbations in the alongshore flow off Oregon are well correlated with the local wind (Huyer and Smith, 1978). However off Peru fluctuations in the alongshore flow do not correlate well with the local wind. Smith (1978) relates that fact to the presence of a poleward-propagating, wavelike perturbation along the Peru coast. The presence and effects of shelf waves and Kelvin waves on upwelling areas is also discussed by Cutchin and Smith (1973), Brink et al (1978) and Allen and Romea (1980).

A poleward undercurrent is an ubiquitous feature of the shelf circulation in upwelling regions. In an early theoretical study, Yoshida (1967) explained the relation of the poleward undercurrent to upwelling. This relation has been widely confirmed by observations (Smith, 1974; Brink et al, 1980). Suginohara (1974), from theoretical considerations suggested that the occurrence of a poleward undercurrent is delayed for a few days after the onset of the wind because of the generation of continental shelf waves. Observations support the idea that the undercurrent intensifies after upwelling events relax (Mooers and Allen, 1973).

#### B. Organization of this Thesis

This study is organized in four chapters. In Chapter II the data from CUE II and JOINT II and their treatment are described. In Chapter III some events are selected from the time series of wind stress and a general overview of the mean state of the flow and temperature fields during the upwelling season is presented. Within this framework I study the

time response of the velocity and temperature fields during individual events. In Chapter IV, possible momentum balances and forcing mechanisms are examined for both the complete data series and during events. Explanations of the observed patterns are discussed in Chapter V. Conclusions are listed at the end of Chapter V.



## II. DATA SOURCES AND HANDLING

### A. CUEA Experiments

In July-August 1973 an upwelling study was conducted over the Oregon continental shelf (CUE II). Later in March to May 1977 a similar study was carried out off Peru (JOINT II). Details of the data acquisition can be found in the data reports (Halpern et al, 1974; Pillsbury et al, 1974; Enfield et al, 1978; Brink et al, 1978).

For our purpose, data from the midshelf current meter arrays are selected (Fig. 1). Although this yields only one geographical point in each region, the moorings provide a complete velocity profile, from surface to bottom (Table 1). No other moorings provide comparable resolution in the vertical.

A natural horizontal scale on an upwelling area, is the baroclinic radius of deformation,  $R = \bar{H} N f^{-1}$  (see appendix I). Theoretical considerations suggest that the replacement or upwelling occur inside the zone limited by  $R$  (Yoshida, 1955). Although the distance from shore at which mid-shelf current meters are located is comparable for both Oregon and Peru, the relative position of the upwelling itself may extend further offshore in Peru (Fig. 1c). In Oregon the upwelling is concentrated within the first 14 km, off Peru it occurs within the first 20 km.

### B. Data Processing

Currents and temperature were measured with Aanderaa current meters. Errors on those measurements have been estimated to be about  $\pm 2 \text{ cm s}^{-1}$  in currents (Halpern et al, 1974) and  $\pm 0.02^\circ\text{C}$  in temperature (Huyer, 1976).

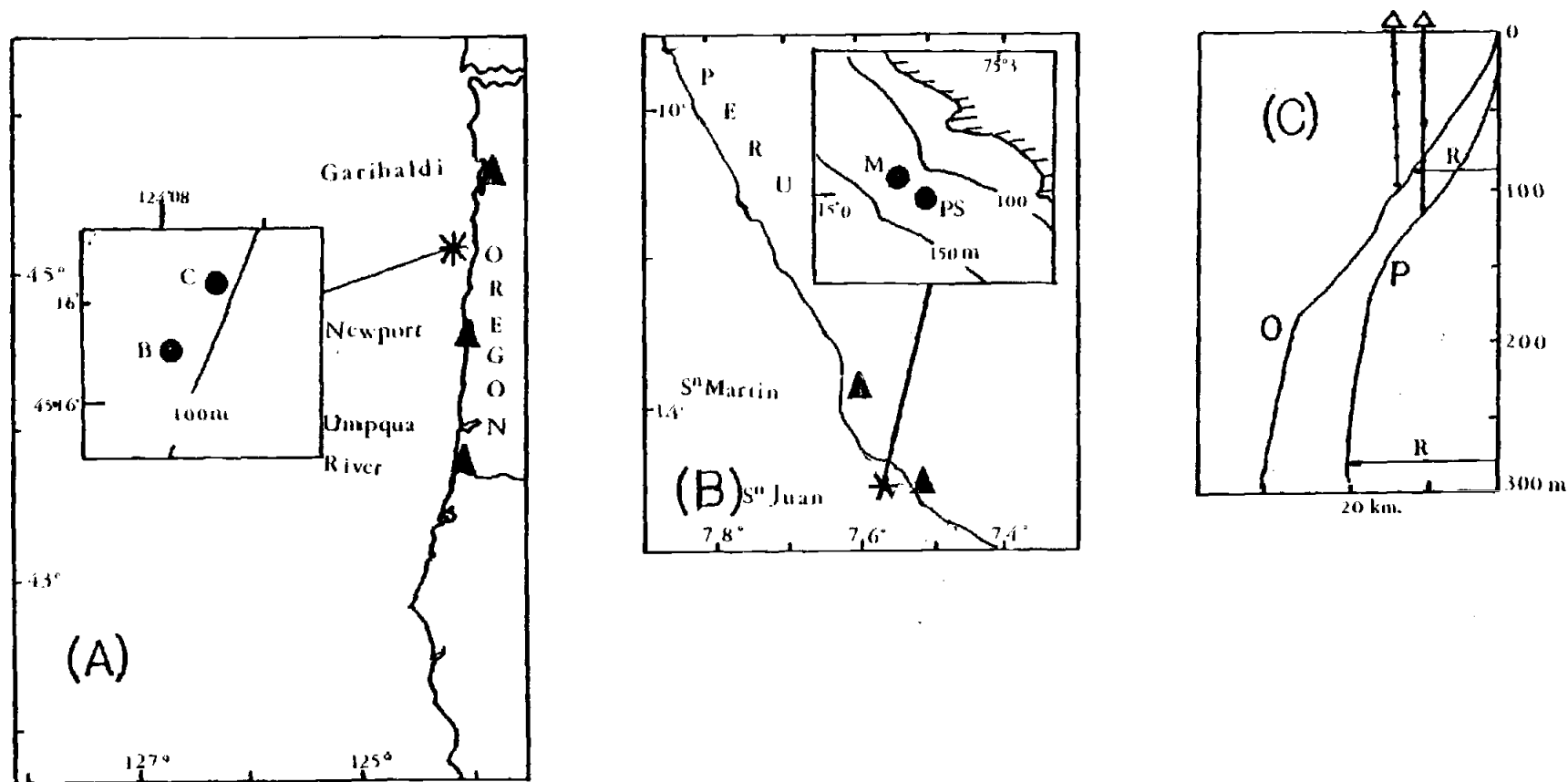


Figure 1 Location of the current meter moorings (●) and tide gauges (▲) during: (A) CUE II experiment off Oregon, July-August 1973; (B) JOINT II experiment off Peru, March-May 1977; (C) configuration of current meter arrays and the estimated baroclinic radius of deformation,  $R$ .

TABLE 1 Description of the data

Area/ experiment	Measurement	Arrays Considered	Position	Distance from shore	Date from / until		Depth of meters	Reference
OREGON	Current	Buoy B	45 15.8 N 124 07.8 W	12 km	July 6 (06 hrs)	Aug. 27 (06 hrs)	0-18.3 m	Halpern et al (1974)
CUE II 1973		Carnation	45 16.2 N 124 06.9 W	11 km	July 2 (00 hrs)	Aug. 27 (06 hrs)	20-95 m	Pillsbury et al (1974)
	Wind	Buoy B	45 15.8 N 124 07.8 W	12 km	July 5 (06 hrs)	Aug. 28 (06 hrs)		
PERU	Current	PS	15 06.8 S 75 30.2 W	12 km	March 7 (06 hrs)	May 13 (06 hrs)	2.6-24	
JOINT II 1977		MILA	15 06.0 S 75 30.8 W	12 km	March 7 (06 hrs)	May 13 (06 hrs)	39-115	Brink et al (1978)
	Wind	PS	15 06.8 S 75 30.2 W	12 km	March 7 (06 hrs)	May 13 (06 hrs)		

All the instruments were calibrated before and after each cruise.

Simultaneously with the current measurements, the wind was measured at the surface buoy (3 m height), with an estimated error of  $\pm 1 \text{ m s}^{-1}$  (Huyer, 1976).

The current meter data, taken at 5 or 10 min. intervals, were first filtered to obtain time series of hourly values; those hourly values were filtered again to eliminate the semi-diurnal and diurnal tides (and inertial oscillations for the case of Oregon). This last filtering process was made by means of a filter spanning 121 hours with a half power point of 40 hrs. (0.6 cpd). The resulting series were decimated to 6 hr. values.

Wind series were filtered by the above process. However, first the wind stress was calculated from the hourly wind components,  $U_W$  &  $V_W$  (see appendix I for notation) according to:

$$\begin{aligned}\tau^x &= \rho_A C_d U_W^2 \\ \tau^y &= \rho_A C_d V_W^2\end{aligned}$$

$C_d$  is a drag coefficient empirically determined as  $1.3 \cdot 10^{-3}$  (Kraus, 1972). The wind stress was also decimated to 6 hr. value series.

Data from coastal tide gauges (Fig. 1) were used to estimate the alongshore pressure gradient. These data were first corrected for the inverted barometer effect (assuming that a pressure increase of 1 mb decases sea level by 1 cm) and then filtered identically to wind and current series. The filtered data may have an error of  $\pm 0.5 \text{ cm}$  (Mooers and Smith, 1968).

The definition of the coordinate system represents a problem in upwelling studies. Simple methods to define the alongshore and onshore direction, such as following the coast line or the orientation of the isobath, have been used. Another way to define the coordinate axes is to determine the principal components of the low frequency fluctuations of the flow over the shelf, and use this to define the two axes. Allen and Kundu (1978) computed the principal components of the velocity off Oregon. The major principal axes deviate from north by only a few degrees. Therefore, the geographical (N-S, E-W) coordinate system is used to describe the flow regime off Oregon. Brink et al (1978), by a similar method, show that off Peru the best set of coordinates result from the rotation of the axis  $45^\circ$  to the left of the geographical coordinates. Therefore data of currents and wind for Peru were rotated according with the transformation law for cartesian tensors. Thus, the alongshore/onshore directions are: towards N & E off Oregon and NW ( $315^\circ$ T) and NE ( $45^\circ$ T) off Peru.

### III. TIME AND DEPTH DEPENDENT CHANGES OF FLOW AND TEMPERATURE FIELDS DURING UPWELLING EVENTS

#### A. Selection of Wind Events

During CUE II, the alongshore component of the wind stress off Oregon had negative values most of the time (Fig. 2). Negative values represent equatorward winds, which are the upwelling favorable winds.

Off Oregon, I selected three events and one anti-event from periods when the magnitude of the alongshore component of the wind stress differs from its average by more than one standard deviation (Table 2). In the first event the wind stress shifted from zero to a negative peak in three days. In this particular event the wind reached the maximum equatorward values for the complete record ( $-3.0 \text{ dynes cm}^{-2}$ ). The second event selected is the longest one, although the wind does not increase as fast as in the first one. In the third event the wind shifted from a maximum poleward to a maximum equatorward in two days and then decrease to zero, also in two days. Between 23 and 25 of August the wind stress was positive; this is the case of an antievent over the Oregon shelf.

In contrast, off Peru the wind stress was equatorward all the time (Fig. 2). Although the wind off Peru was always favorable to upwelling, fluctuations in its intensity do occur. From these fluctuations I randomly selected three events for analysis (Table 2).

The selection criteria for Peru were rather arbitrary. I selected three events from periods when the alongshore component of the wind stress was greater than its mean for more than one inertial period. However, in only one of the events was the wind greater than one standard deviation from the mean (event 3).

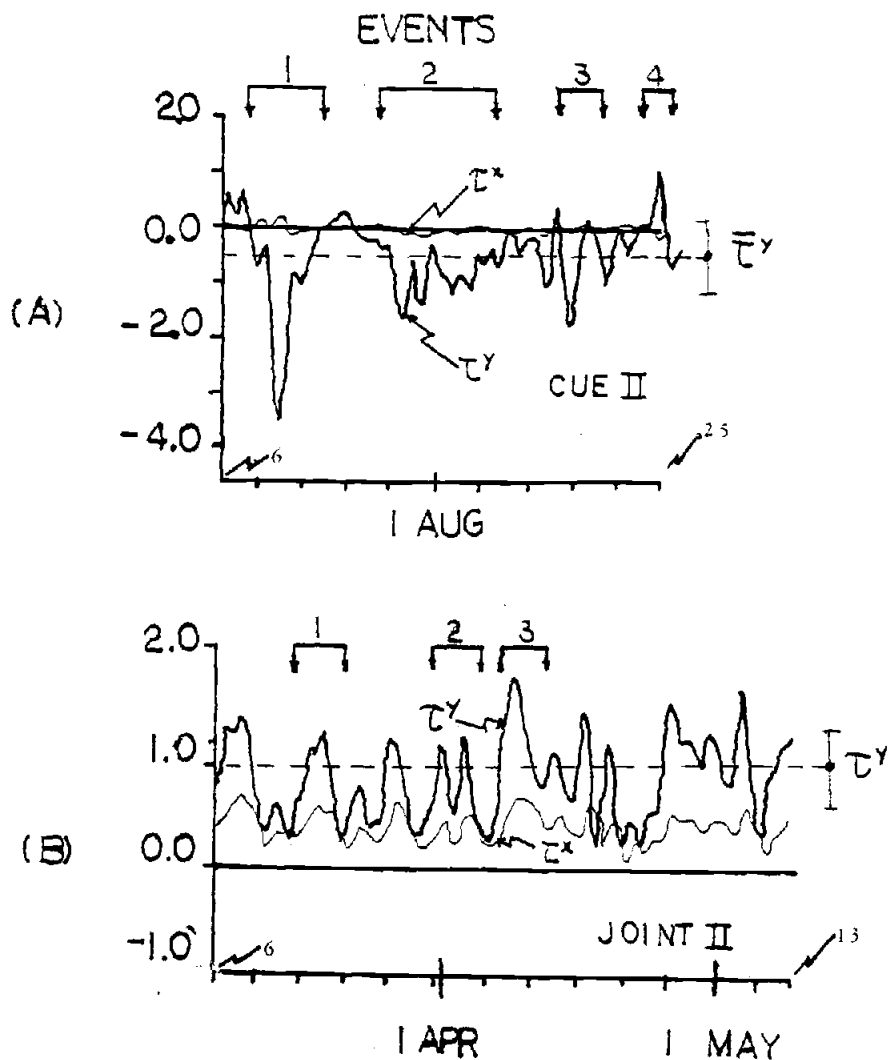


Figure 2 Midshelf values of the wind stress components: (A) Oregon CUE II, July-August, 1973; (B) Peru JOINT II, Mar.-May, 1977. Horizontal dashed lines correspond to mean values of the alongshore wind stress, and vertical bars indicate one standard deviation. Ticks on the time axes indicate 5 days periods.

Table 2. Selected Wind Events

<u>Wind Events off Oregon</u>	<u>From</u>	<u>Until</u>
1	00 hrs. July 9 (1973)	18 hrs. July 17
2	00 hrs. July 25	18 hrs. August 6
3	00 hrs. August 14	18 hrs. August 18
Antievent off Oregon	00 hrs, August 23	18 hrs. August 27

Wind Events off Peru

1	00 hrs. March 14 (1977)	18 hrs. March 20
2	00 hrs. March 29	18 hrs. April 4
3	00 hrs. April 6	18 hrs. April 12



It can be seen, in both areas, that the time between events is not always the same. In general, there is a two weeks period between them.

#### B. Mean Flow Field

Before proceeding to look for details of the response of the coastal waters to the selected wind events, I review some of the more relevant features of the mean flow during the complete series (CUE II and JOINT II).

First I will review a typical profile of the mid-shelf currents. To perform this analysis one can decompose the velocity vector in two orthogonal components. The resulting time series constitute the along-shore ( $v$ ) and the cross-isobath ( $u$ ) components. By this decomposition one tends to separate the fluctuations and dynamics occurring in either direction. From this information vertical profiles were constructed by plotting the mean magnitude of the components of the flow ( $u, v$ ) registered by each current meter at different depth (Fig. 3). The meaning of "mean" from here on corresponds to the "average value" during CUE II and JOINT II.

The basic characteristics of the mean cross-isobath flow during upwelling is an offshore-directed flow in the surface Ekman layer. This pattern can be seen in both areas, Oregon and Peru, where the mean flow is offshore in the upper 20 m (Fig. 3).

The water that is transported offshore is replaced by the upwelled water supplied by an onshore flow. This flow is evident below 20 m for both Oregon and Peru.

The question now is does the onshore transport below 20 m compensate that which is moved to the open ocean in the surface layer? A simple

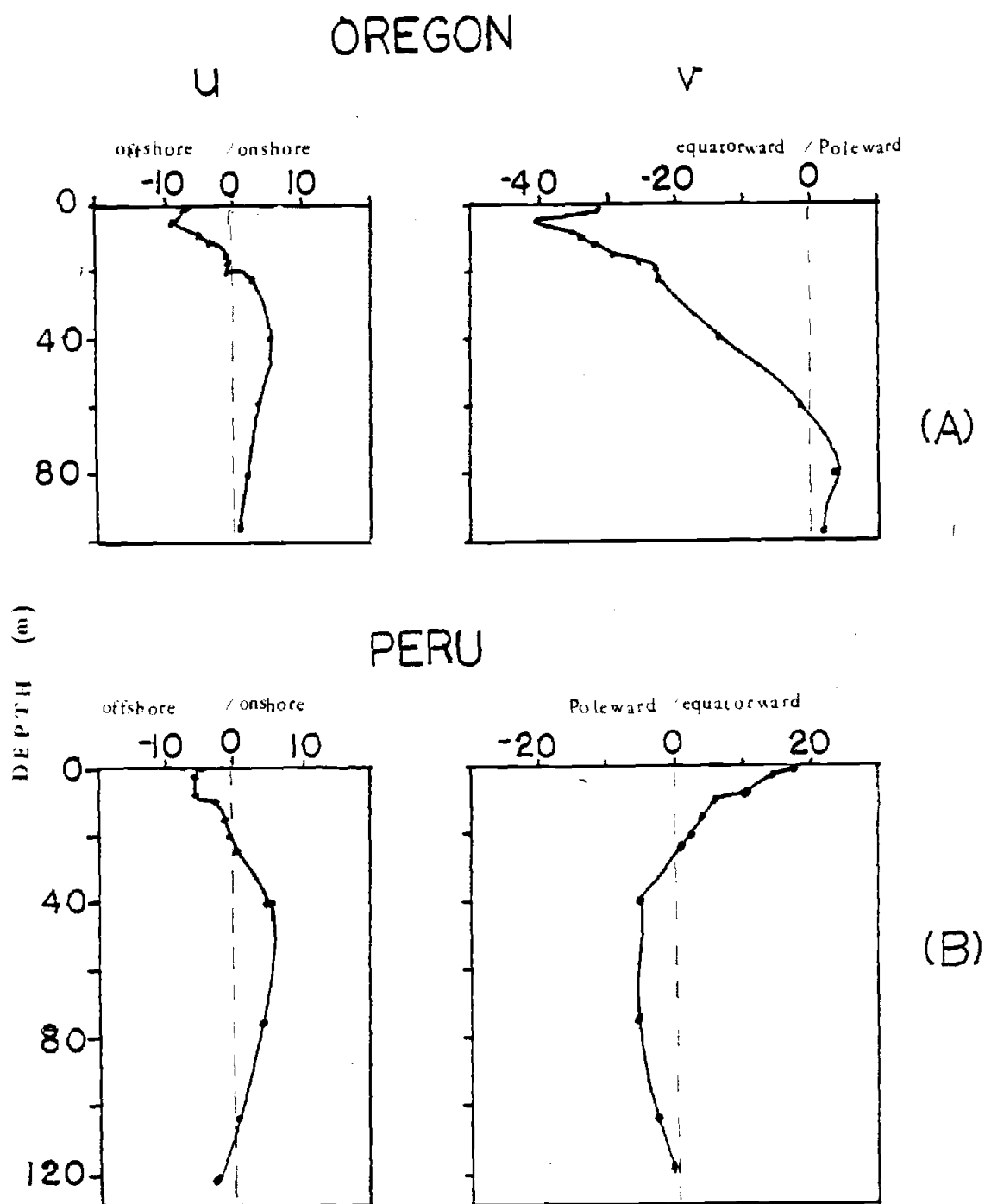


Figure 3 Mean current profiles for the midshelf current meter array off ; (A) Oregon and (B) Peru (6 July to 27 August 1973 for Oregon and 22 March to 10 May 1977 for Peru).

examination of Fig. 3 suggests a negative answer. Further discussion of the two-dimensionality of the volume budget is given in IV D.

While the mean onshore/offshore flow was quite similar in Oregon and Peru, the mean alongshore flow is not so similar. Off Oregon there is a strong and thick (60 m) equatorward flow. It may be part of the coastal jet theoretically predicted for an upwelling area. (Yoshida, 1955; Allen, 1973). On the other hand, off Peru the thickness (20 m) and the strength of the equatorward flow is considerably less than off Oregon, while the poleward flow extends over a much thicker zone than off Oregon and dominates most of the water column.

#### C. Variability in the Flow and Temperature Fields

The emphasis of this thesis is on the pattern of variability associated with wind events. To analyze the variability, the time series of the two components of the flow are studied at two specific depths (3.4 m and 80 m off Oregon; 4.6 m and 80 m off Peru) and compared with the fluctuations of the wind.

In the upper layer off Oregon (3.4 m) the offshore and the equatorward flow both intensify during events (Fig. 4a). During events 1 and 2 the u and v components were larger than one standard deviation from the mean. During the antievent off Oregon the response of the currents was also strong, but appeared as an onshore flow which is characteristic of a downwelling situation.

The current meters also registered temperature at the different levels. Since the temperature provides a good representation of the density field, it is relevant to study changes in the thermal conditions

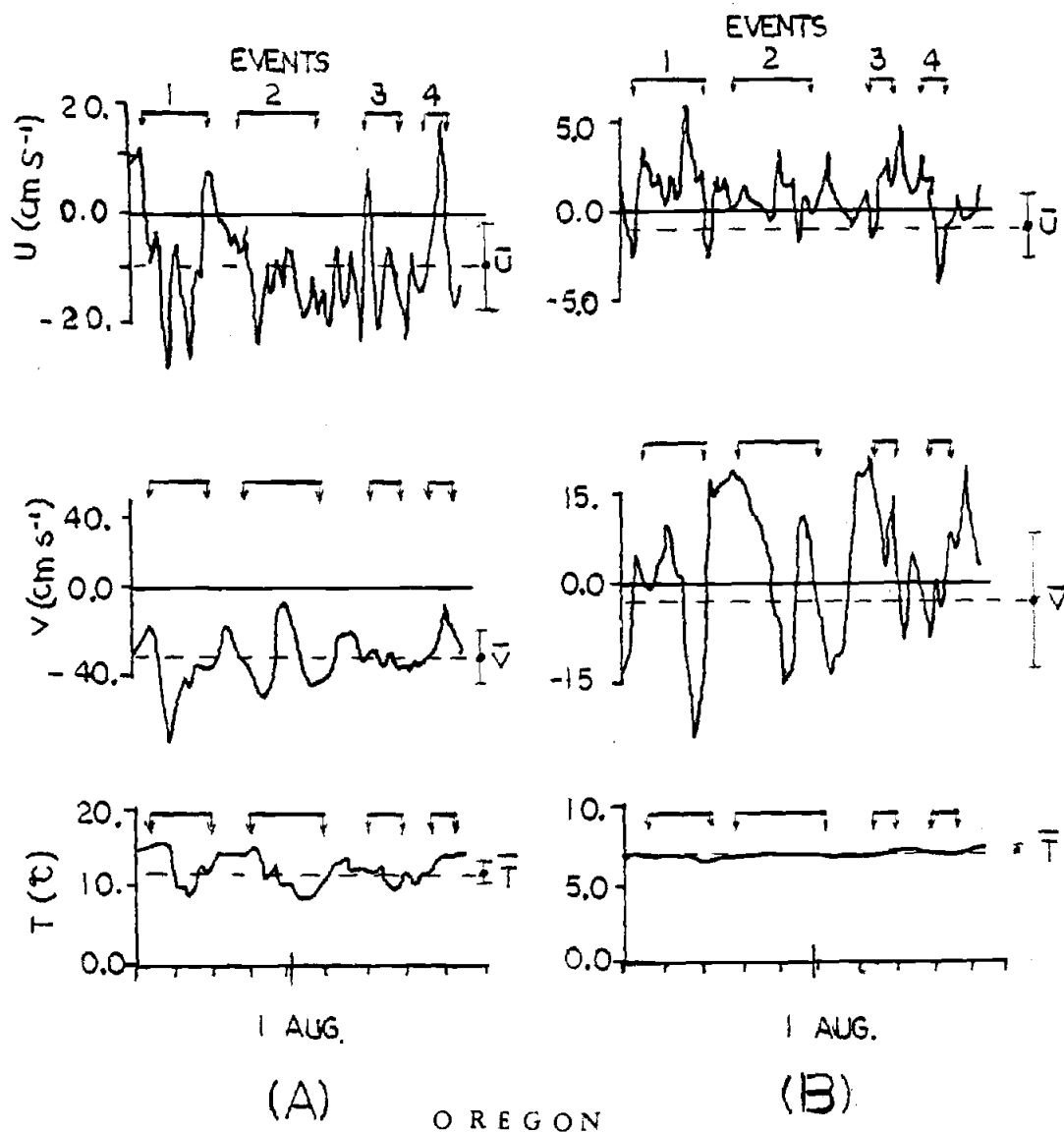


Figure 4 Complete time series of velocity and temperature for CUE II from: (A) surface (3.4m) and (B) near the bottom (80m). Ticks on the time axes indicate 5 days periods.

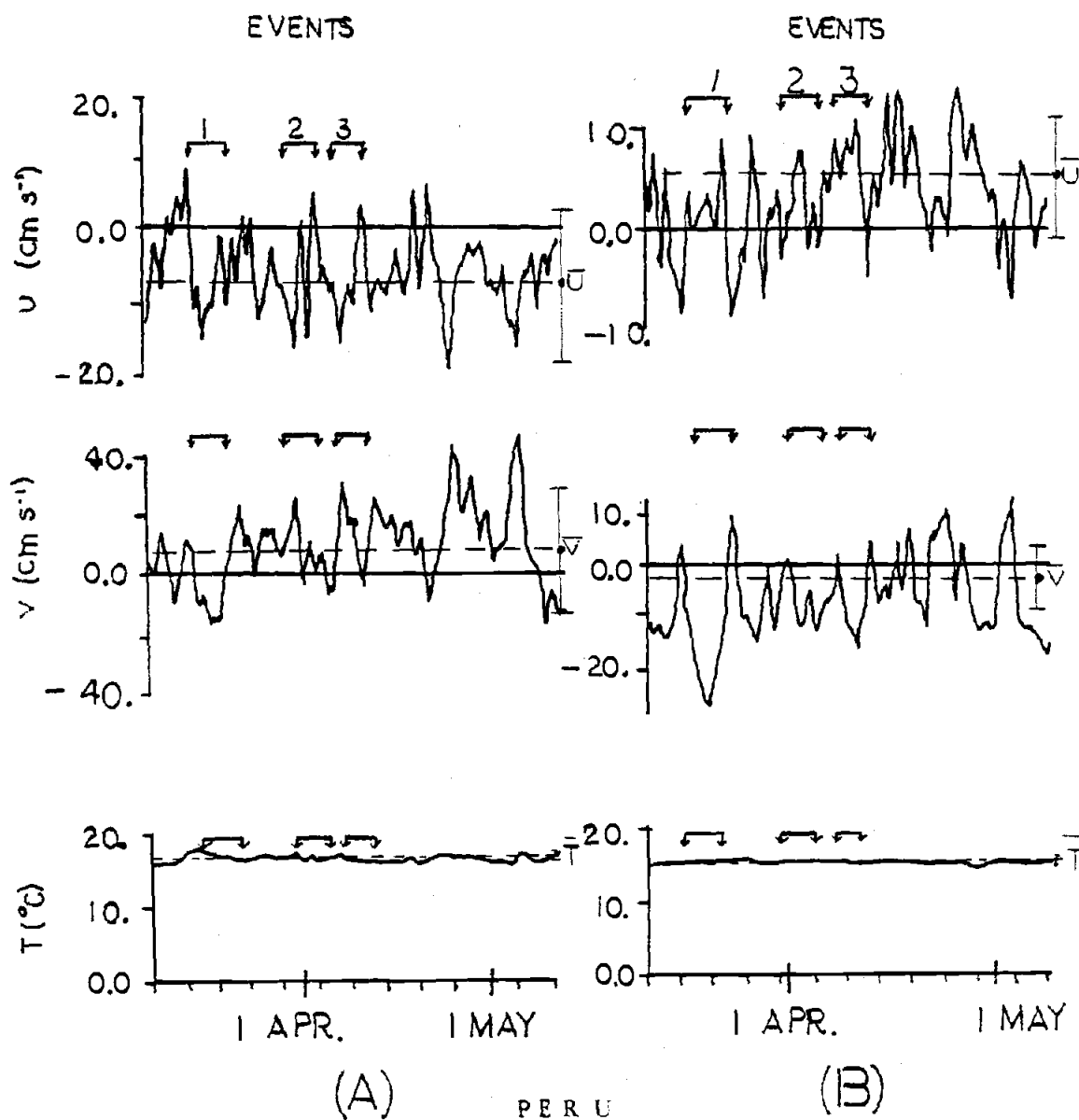


Figure 5 Complete time series of velocity and temperature for JOINT II from: (A) surface (4.6m) and (B) near the bottom (80m). Ticks on the time axes indicate 5 days periods.

as a response to the wind events (Fig. 4). The upwelled waters, coming up from the deeper layers of the coastal ocean are relatively colder. One can expect that the temperature at the surface layer should get colder during events and that is exactly what happens (Fig. 4). The thermal fluctuations on the surface, were larger than one standard deviation from the mean. On the other hand, during the antievent, the water is moved towards the shore by the wind drift. The results show that the water temperature increased during the antievent, reaching a value of  $14^{\circ}\text{C}$  (Fig. 4a), which appears to be a normal temperature for periods of positive wind stress off the Oregon Coast (see Fig. 2).

In addition, at 80 m depth the flow also changes during events (Fig. 4b). The cross-isobath flow,  $u$ , increases in the onshore direction in events 1, 2, and 3. During the antievent it is directed offshore. In the middle of events 1 and 2, the alongshore flow,  $v$ , was equatorward, and at the end of the same events it shifted to poleward (positive values). The temperature does not fluctuate at 80 m as it does at the surface, where the stratification plays an important role.

Off Peru the flow is more variable than off Oregon (Fig. 5). In fact, the standard deviations of both flow components are larger in Peru than in Oregon. During events the flow is offshore in the surface (4.6 m) and onshore in the interior (80 m). The surface alongshore flow off Peru was poleward in event 1, but equatorward during the other two events.

Changes in temperature associated with events were much less significant in Peru than off Oregon. This is a consequence of the differences in stratification between the two zones. Off Oregon the

average stratification at mid-shelf is four times greater than off Peru (Smith, 1980). In the surface layer off Peru, a small decrease on the temperature values is noticeable during events but as off Oregon, changes in the bottom temperature are not perceptible.

#### D. Flow Fields During Events

##### D.1. Oregon

In the previous section I discussed the general nature of departures of  $u, v$ , and  $T$  from the mean during events. In this section I discuss the relation between the wind stress and the flow in the water column during events.

The first pattern noted off Oregon is that when the upwelling favorable wind stress increases, a simultaneous peak occurs in both flow components (Fig. 6a - 6c). The three events off Oregon present common patterns.

A maximum offshore flow in the upper 10 m, occurs almost simultaneously with the maximum wind. At the same time, the interior inshore flow reaches a maximum. The layer with offshore-directed flow is relatively thin, less than 20 m in all events off Oregon. However the layer with onshore flow was at least 80 m thick.

The alongshore flow at the beginning of events is equatorward as in the mean state (Fig. 6a - 6c), but a short time after the wind becomes strong, it increases considerably. The strongest flow occurs in the surface but it increases gradually with time in all the water column. However, two or three days after the maximum wind a poleward flow appears below 30 m depth. By this time, the wind was in general relaxing, i.e., the values of the wind stress fall back inside of the envelope formed

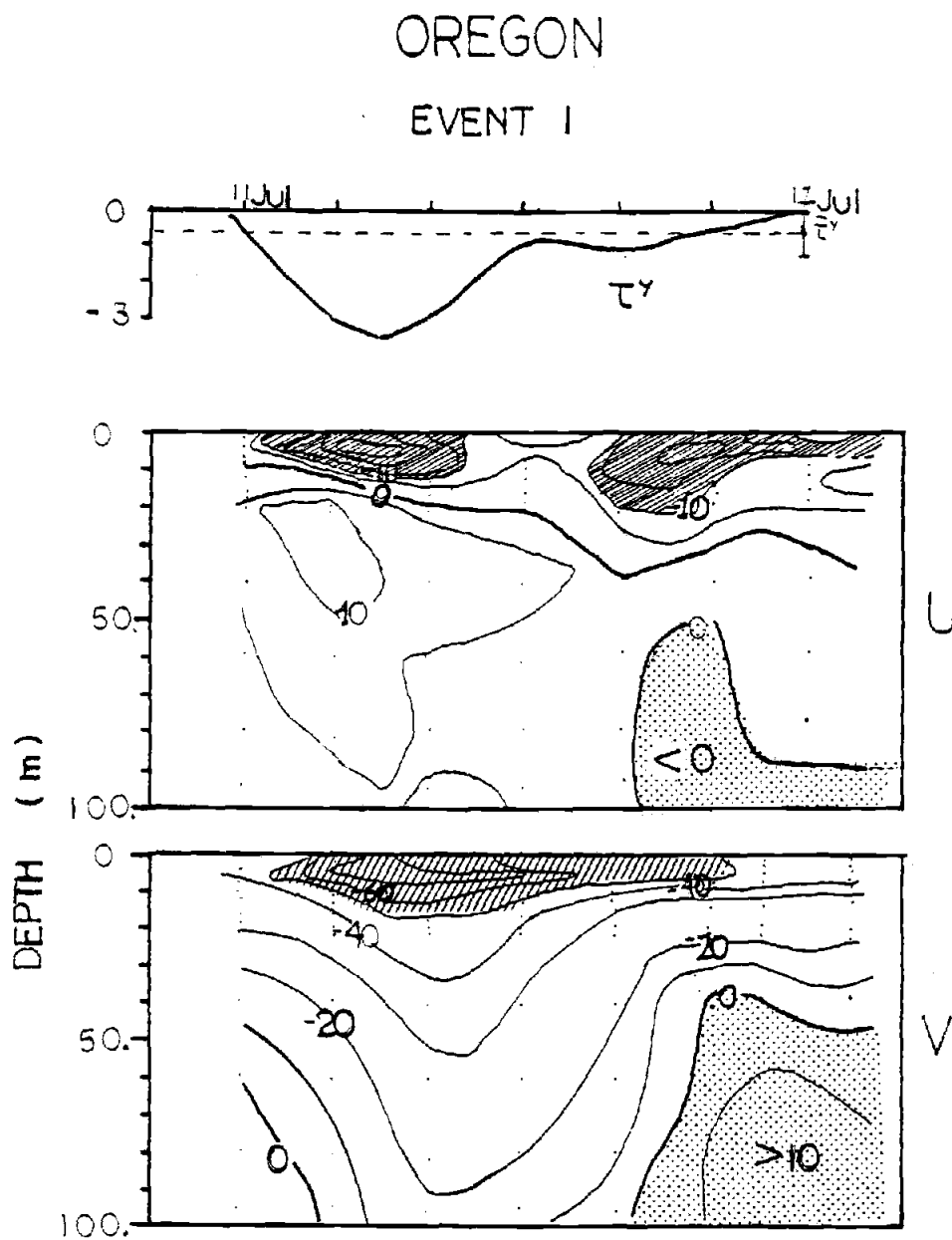


Figure 6 Time-depth sections of velocity off Oregon during events (a-d), together with the wind stress and its overall mean and standard deviation. Different shaded areas indicate surface offshore-equatorward flow and deep offshore-poleward flow. Contour intervals are: 5 cm/s for  $u$  and 10 cm/s for  $v$ .



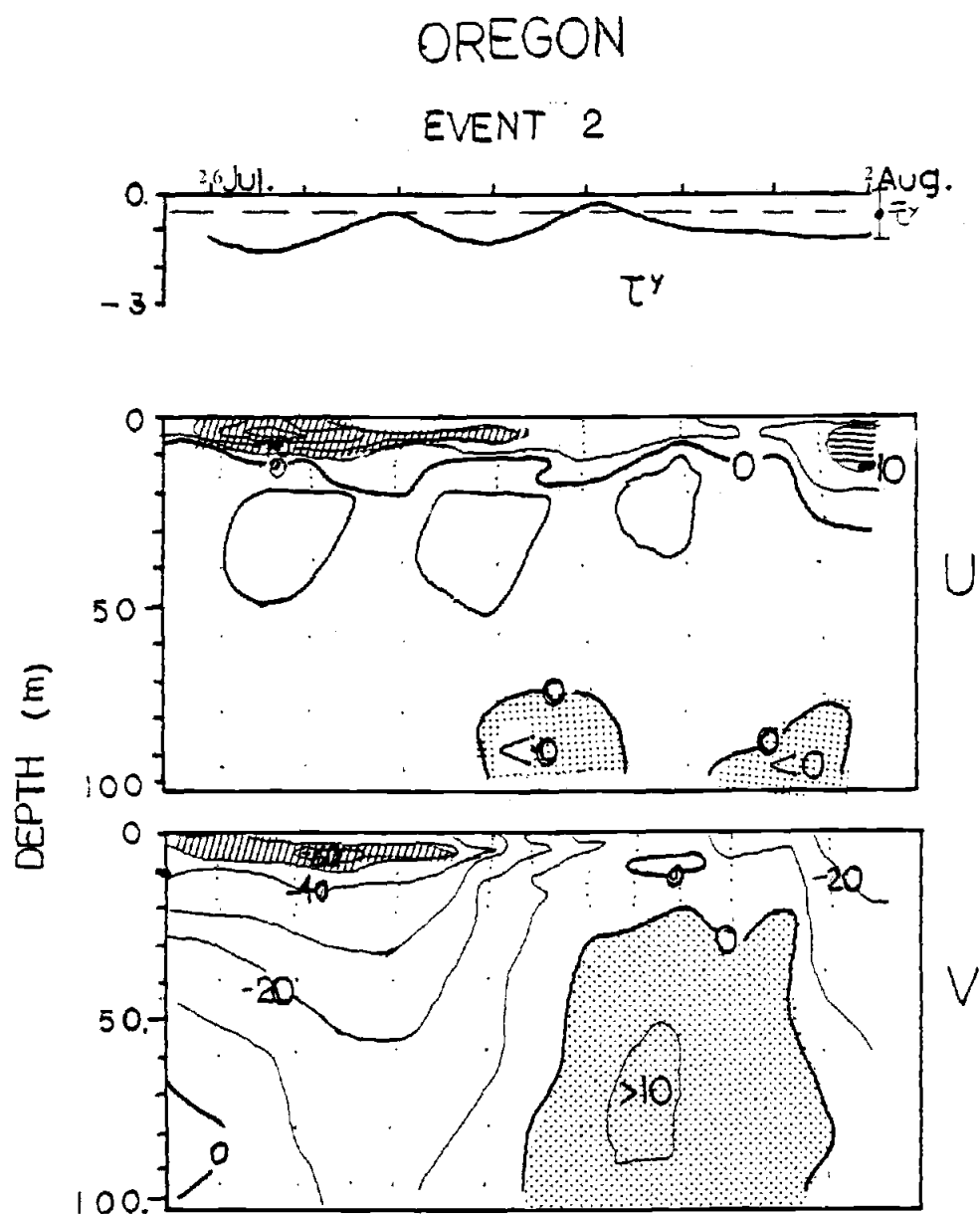


Figure 6b

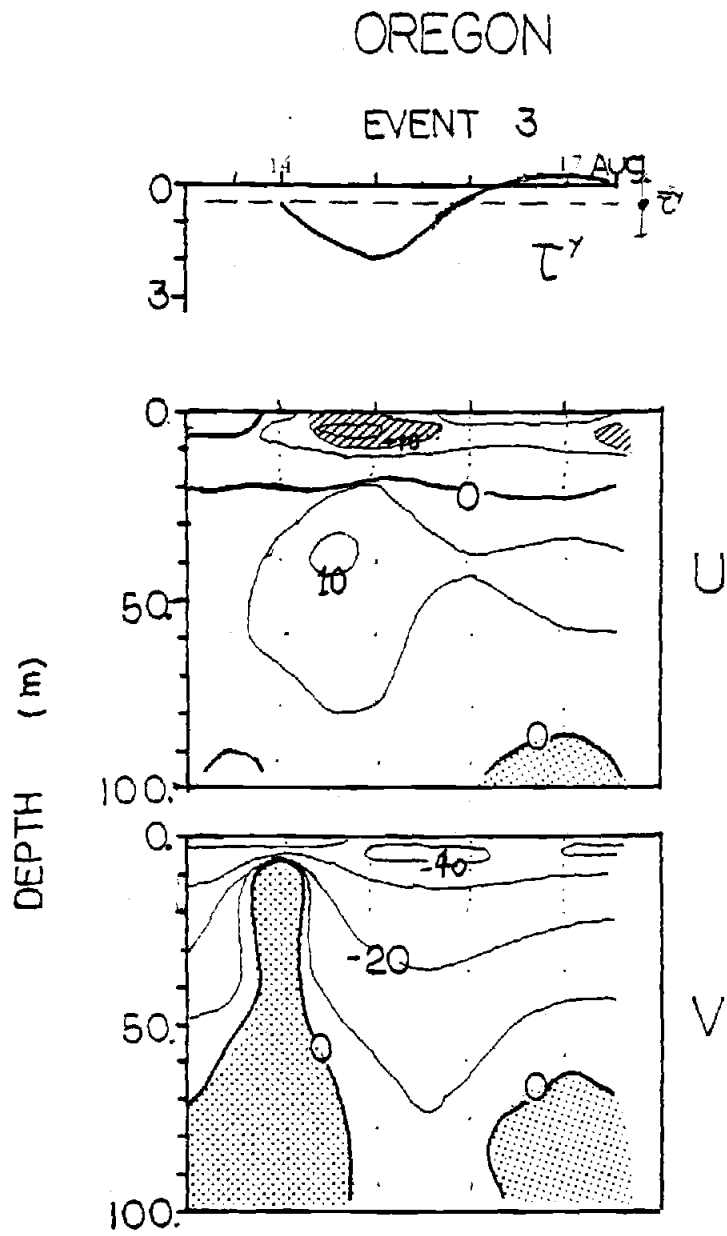


Figure 6c

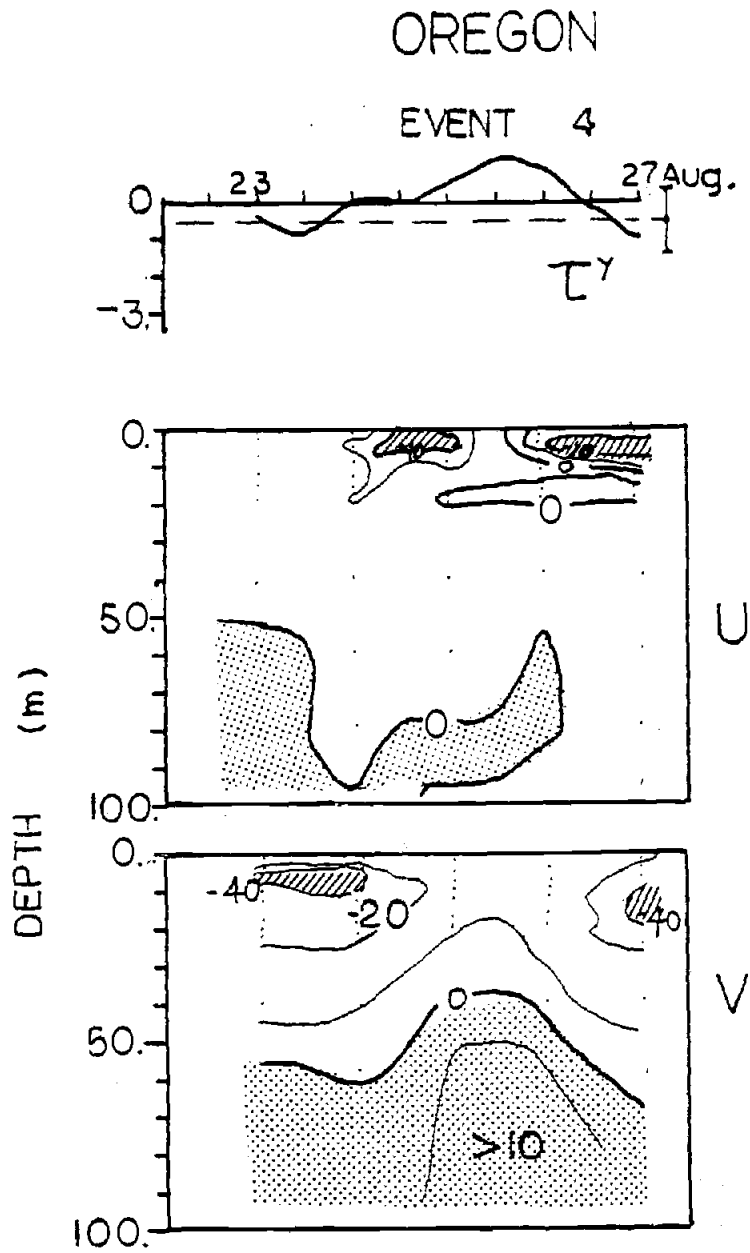


Figure 6d

by the standard deviation about the mean. An additional feature occurs during event 3 off Oregon; a poleward flow is present at the beginning of the events and virtually disappears with the maximum wind (Fig. 6c).

Associated with the poleward flow, offshore flow adjacent to the bottom is apparent in the profile for the u component. The presence of this pattern in all the three events suggests that the poleward flow causes a bottom Ekman layer.

The antievent presented characteristics expected for a downwelling situation. In the middle of the upwelling season off Oregon the wind suddenly turned to poleward between August 23 and August 27 (Fig. 2). The response of the currents was distinguishable in all the water column. In the surface layer the offshore flow diminished as the maximum wind is approached (Fig. 6d). The equatorward flow that was initially present disappears from the surface layer with the poleward wind. Accompanying this period, the poleward undercurrent intensify between the bottom and 50 m. Later, when the wind is restored to its mean values both the offshore and the equatorward flow are also restored to the pre-event status.

#### D.2. Peru

Off Peru, as off Oregon, there is an immediate increase in the offshore flow accompanying the peak of the wind (Fig. 7a - 7c); a similar statement describes the case of the interior onshore flow.

The alongshore flow, is not always equatorward in the surface. In event 1, even when the wind was intense and equatorward, the surface current was poleward, i.e. against the wind. In that occasion the poleward flow is found throughout the water column during the complete

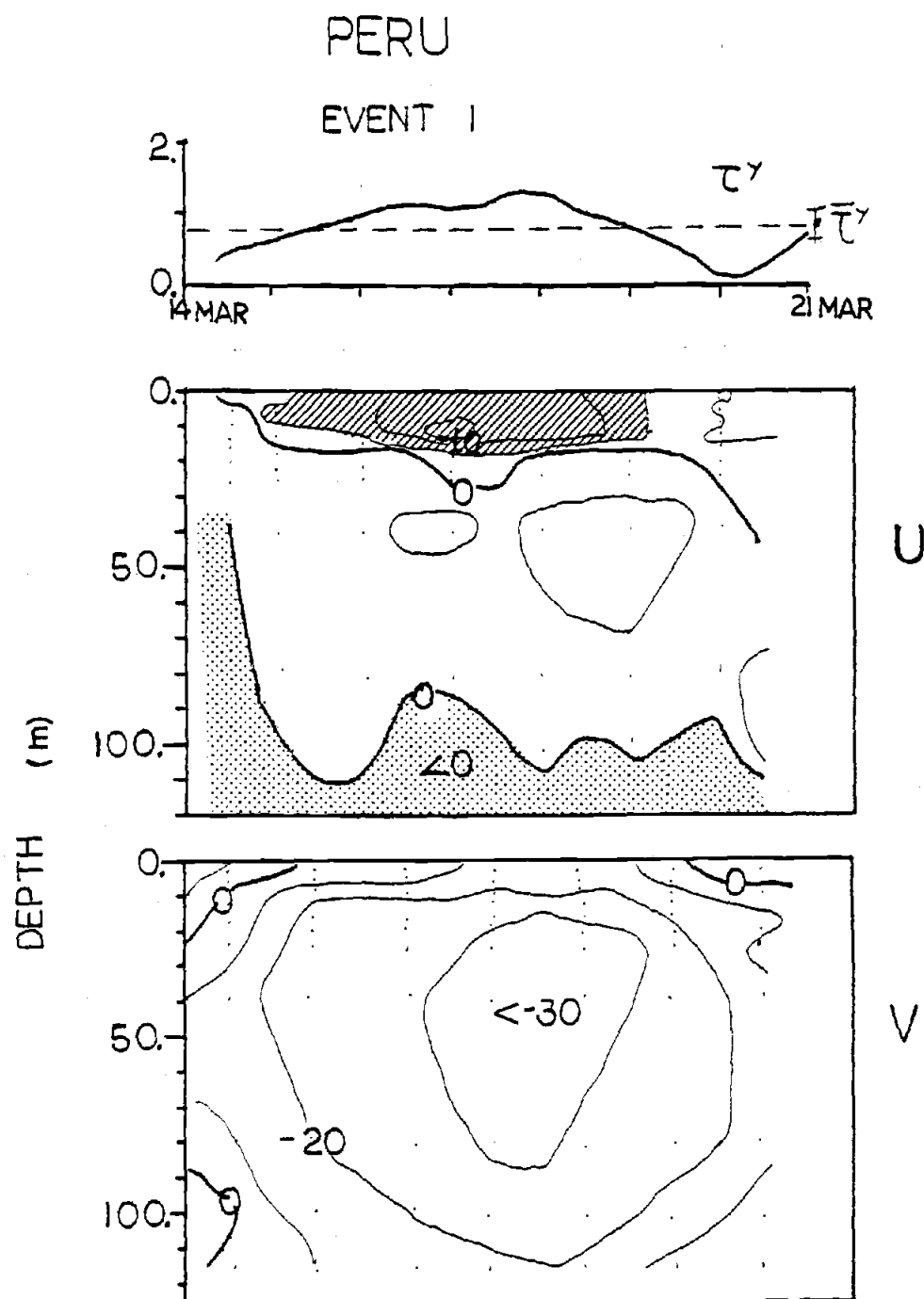


Figure 7 Time depth sections of velocity during events off Peru (a-c), together with the wind stress and its overall mean and the standard deviation. Shaded areas indicate surface offshore-equatorward flow. Contour intervals are: 5 cm/s for  $u$  and 10 cm/s for  $v$ .

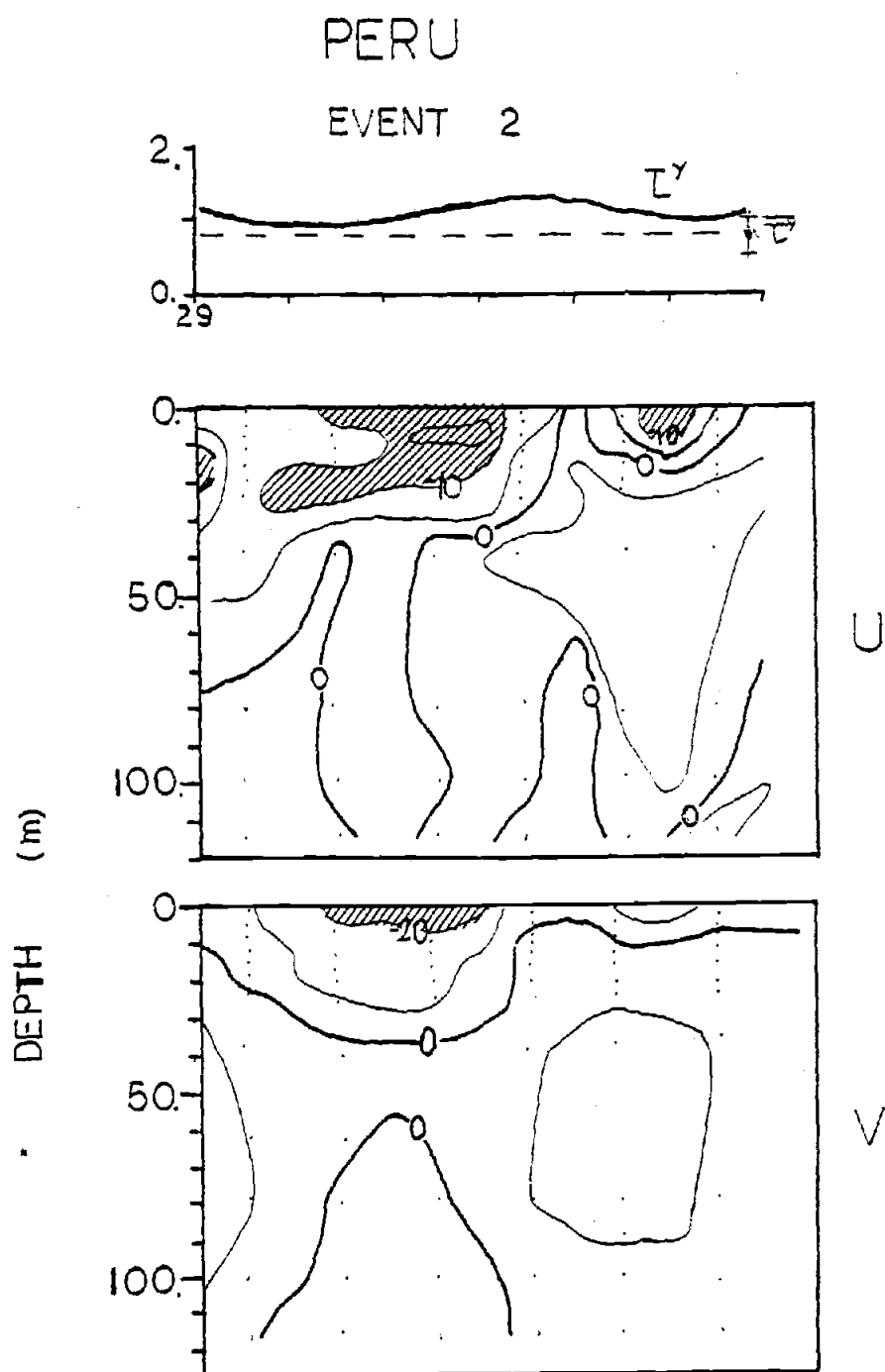


Figure 7b

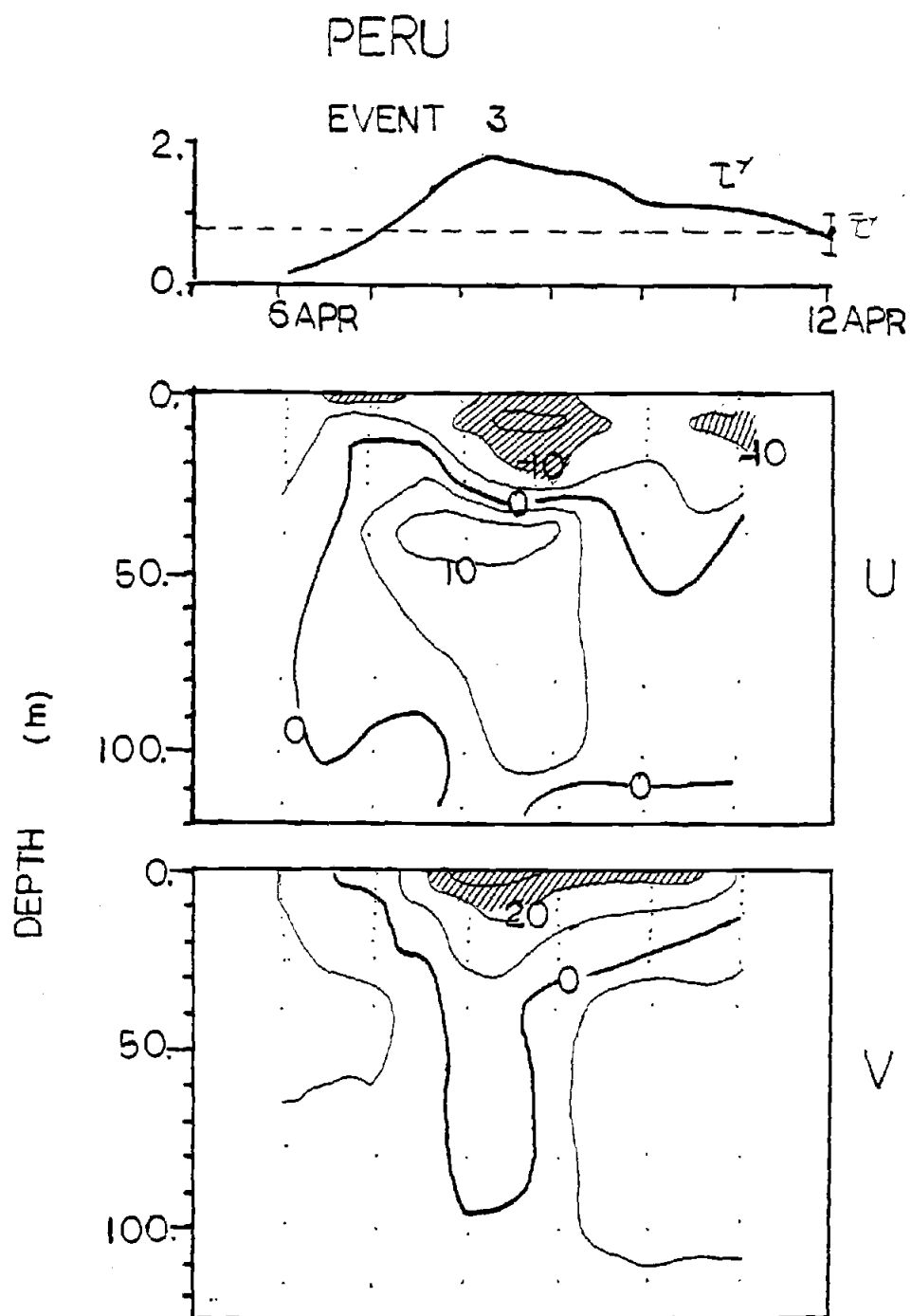


Figure 7c

event. The core of maximum negative  $v$  was centered above 30 m depth and its speed was about  $-30 \text{ cm s}^{-1}$ . During events 2 and 3, the alongshore flow was equatorward (as the wind), but only in event 3 is its maximum value simultaneous with the maximum wind stress.

#### E. Time Lags

While the previous sets of graphs (Fig. 6, 7) are suitable to study trends during events, they do not reveal quantitative details on time lags between wind and currents. The time lag aspect is better studied by analyzing time plots of each variable ( $u$ ,  $v$ ,  $T$ ) at specific depths. Here I select two depths 3.4 m (4.6 m off Peru) surface and an 80 m bottom level. Results are shown in Figs. 8 to 11.

This method of presenting event data supports the previous descriptive analysis. The maximum offshore flow and the maximum wind (dashed vertical lines) are indeed simultaneous in all three events (Fig. 8). Generally the alongshore component maximum lags the wind stress maximum, and the temperature takes even more time to respond fully to the wind.

In the surface waters, small fluctuations of the wind stress on events 1 and 2 are reflected also in small changes in  $u$ . This is not the case for either  $v$  or  $T$ . In fact, the  $u$ -component tends to follow the wind closely.

During the antievent, the maximum onshore flow actually precedes the maximum wind, and the equatorward flow reaches a minimum before the maximum poleward wind.

At 80 m level (Fig. 9) changes associated with events are seen in both  $u$  and  $v$ -components. However, the temperature stays fairly uniform all the time. In all three events, the onshore flow has a maximum almost



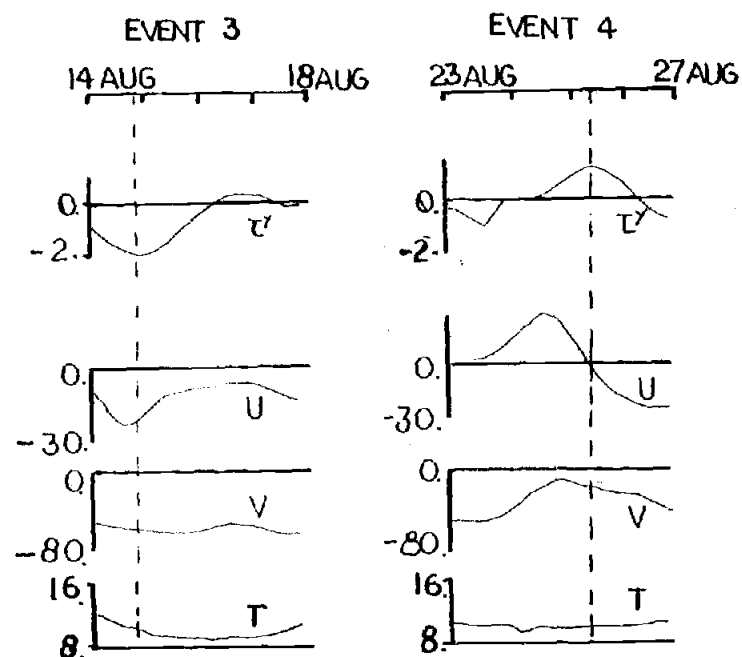
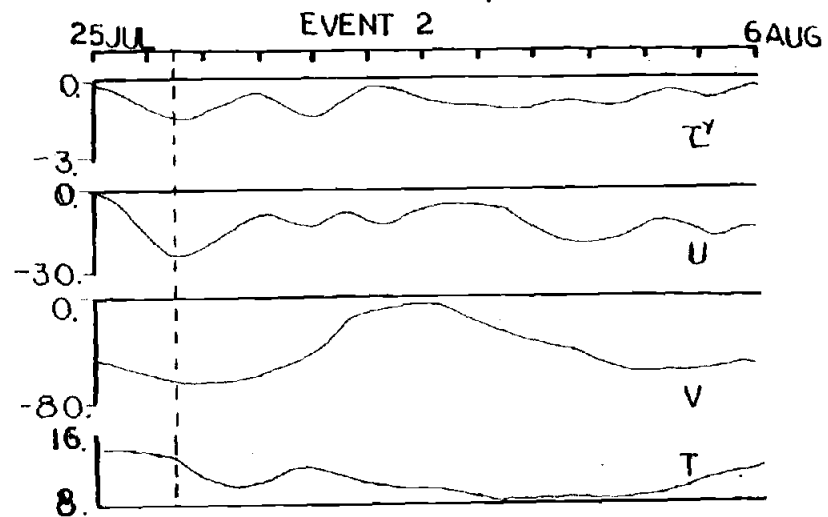
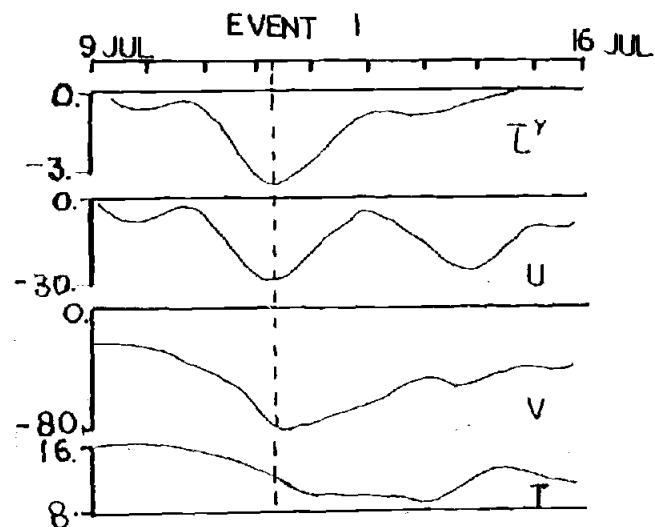


Figure 8 Time series of alongshore wind stress (dynes/cm<sup>2</sup>), velocity components (cm/s) and temperature (°C) for events off Oregon at 3.4m. Dashed vertical lines indicate time of maximum wind stress.

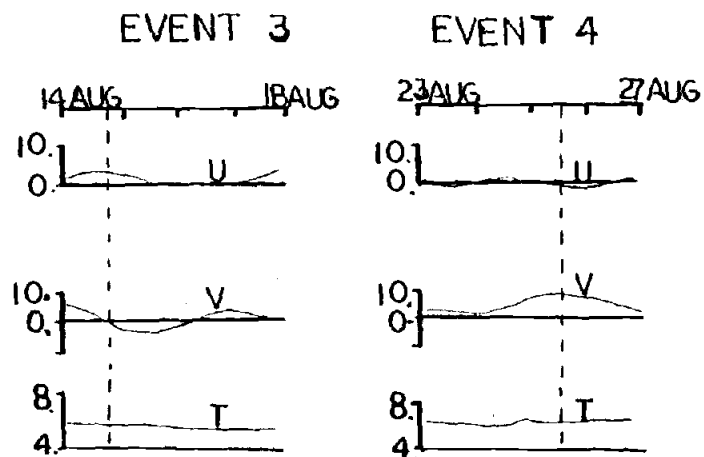
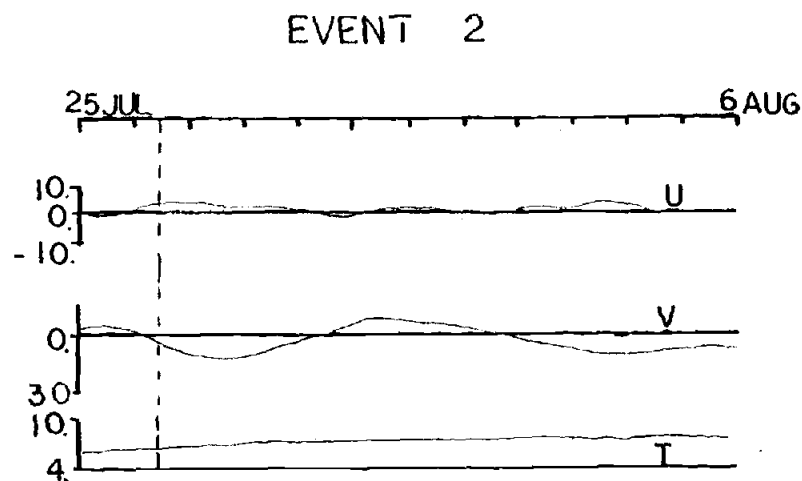
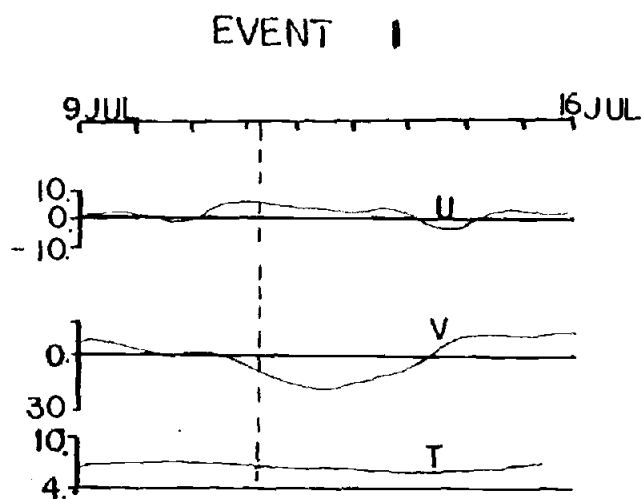


Figure 9 Time series of alongshore wind stress (dynes/cm<sup>2</sup>), velocity components (cm/s), and temperature (°C) for events off Oregon at 80m. Dashed vertical lines indicate time of maximum wind stress.

simultaneous with the wind, but the maximum  $v$  occurs at a longer time lag than at the surface.

Off Peru, as in Oregon, two different depths were selected to follow changes of currents and temperature with time. At 4.6 m the results show that changes accompanying the wind do occur, but the peak values do not coincide as closely with the maximum values of the wind stress (Fig. 10). In addition, the amplitude of the responses are less than off Oregon. Off Peru, the three variables ( $u$ ,  $v$ ,  $T$ ) are seen to be not as well associated with the wind as is the case off Oregon; therefore the interpretation of the results is difficult.

The maximum offshore flow tends to lead the wind in events 1 and 3; similarly, the alongshore component also tends to precede the wind in events 1 and 3. On the other hand, at 80 m depth (Fig. 11), the magnitude of the fluctuations of the flow are less than in the surface, and temperatures remain unchanged.

Tables of time lags were prepared to summarize the information for Figures 8, 9, 10, and 11. Values of these lags were calculated by taking four points around the peak values and using a four-point parabolic fit one finds the time of the maximum (Tables 3, 4). Averaging the lag values represents the simplest way to summarize the information. Caution should be used in interpreting the time lags, these were computed using low-pass filtered data decimated at 6 hour intervals.

The time lags between the maximum wind and the peak values of the flow and temperature, off Oregon, are puzzling (Table 3). However, maximum of the  $u$  components do occur almost simultaneously with the maxima of wind. Considering the filtering applied to the data and the 6 hr. interval, the average value (-2.6 hrs.) is not much different from

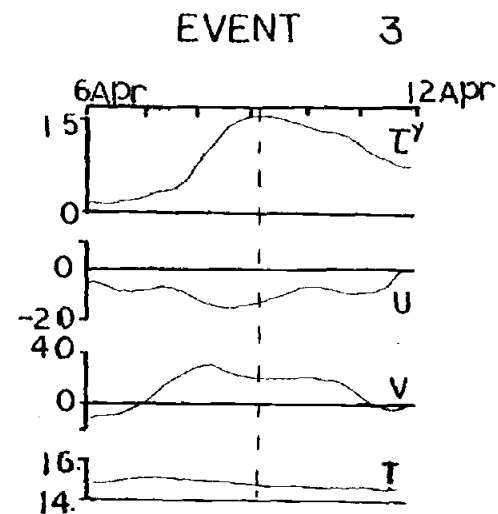
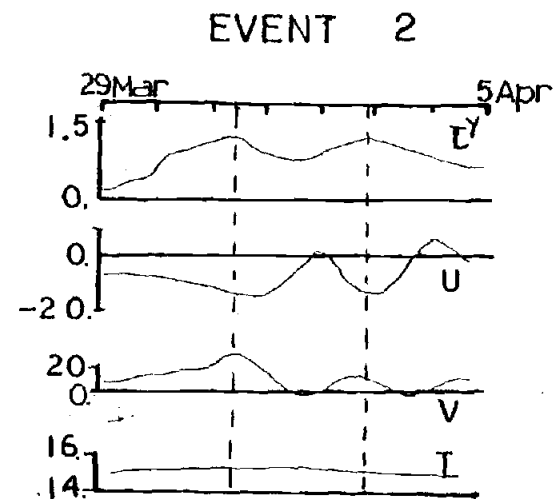
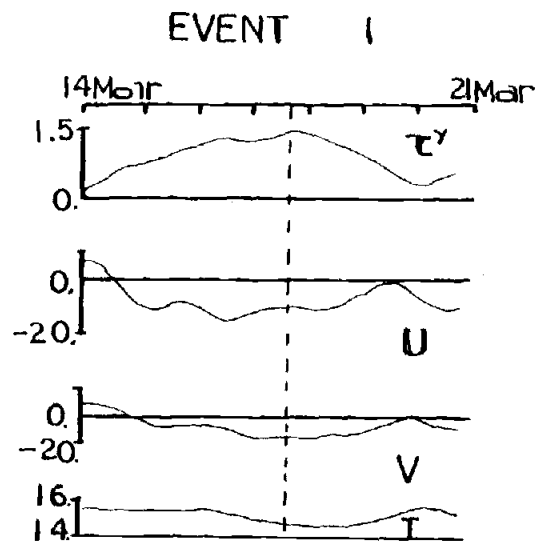
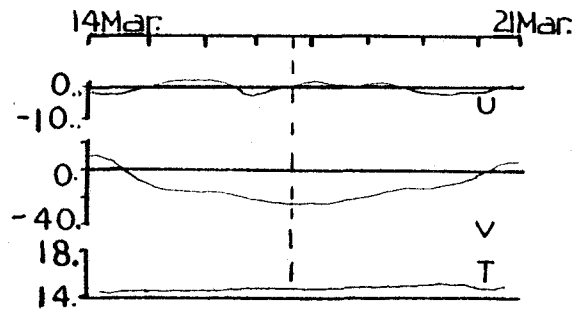
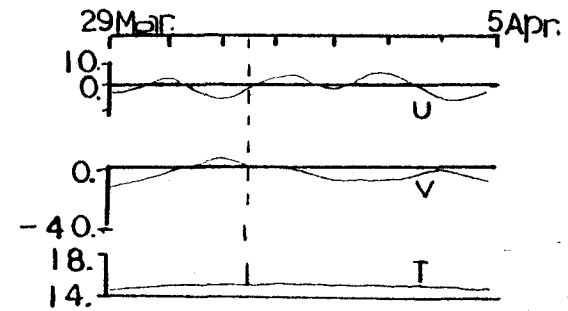


Figure 10 Time series of alongshore wind stress (dynes/cm<sup>2</sup>), velocity components (cm/s), and temperature (°C) for events off Peru at 4.6m. Dashed vertical lines indicate time of maximum wind stress.

### EVENT 1



### EVENT 2



### EVENT 3

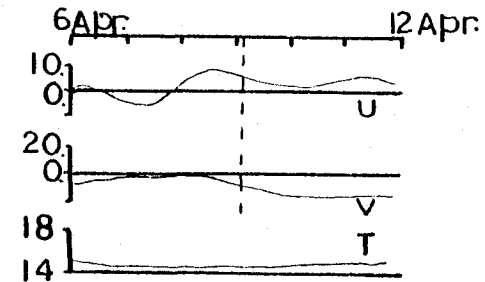


Figure 11 Time series of alongshore wind stress (dynes/cm<sup>2</sup>), velocity components (cm/s), and temperature (°C) for events off Peru at 80m. Dashed vertical lines indicate time of maximum wind stress

zero. On the other hand, changes in the alongshore component of the flow occur in a time in the order of the inertial period, which for Oregon is 16 hrs.; with the exception of the first event in which the lag is less (+4 hrs.). In the latter case the strong wind may be the cause for the shortening of the lag. Temperature lags in the near surface layer average about 1 day.

At the deeper level (80 m) flow and temperature time lags are larger than at the surface, especially for temperature. However, the maximum onshore flow is simultaneous with the maximum offshore flow and the wind.

For the antievent, the response times were calculated for the maximum onshore flow, minimum equatorward flow, and the maximum surface temperature. All the peak values precede the maximum wind significantly (Table 3). The maximum in the surface u component and in temperature tends to occur almost a day before the maximum wind.

A similar lag table was prepared for the poleward flow off Oregon (Table 3). The poleward flow generally appeared at a lag between two or three days, and reached its maximum within approximately four days following the peak in the wind stress. Hence, the poleward flow is characteristic of the relaxation of upwelling events.

Similar lag tables were prepared for Peru (Table 4). For the evaluation different considerations were made. Relative values considered in each case are shown under each table.

No clear tendency is evident from Table 4. In general, time lags off Peru are erratic and larger than off Oregon. At the surface both flow component responses tend to precede the wind. At 80 m (Table 4) not

Table 3. Time lags (hrs.) between maximum wind stress and maximum (minimum) values of variables off Oregon. Calculations were made using 4-point parabolic fit to define times of occurrence of peaks.

CUE II - Response at 3.4 m

<u>Event</u>	<u>1</u>	<u>2</u>	<u>3</u>	<u>Average</u>	<u>Antievent</u>
u	-3	+1	-6	-2.6	-21
v	+4	+13	+16	+11	-12
T°	+22	+18	+36	+25	-27

CUE II - Response at 80 m

<u>Event</u>	<u>1</u>	<u>2</u>	<u>3</u>	<u>Average</u>	<u>Antievent</u>
u*	-4	+4	-2	-0.7	#
v**	+23	+19	+16	+19	-2
T°	+53	+60	+10	+41	-5

\* for maximum inshore flow

\*\* for maximum equatorward flow

# not significant change ( $u \approx 0$ )

CUE II - Response of the Poleward Flow During Events

<u>Event</u>	<u>1</u>	<u>2</u>	<u>3</u>
First appearance	+72(3.2 d)	+70(2.9 d)	+34(1.4 d)
Reaches maximum	+124(5.2 d)	+96(4.0 d)	+52(2.1 d)

Table 4. Time lags (hrs.) between maximum wind stress and maximum (minimum) values of variables off Peru. Calculations were made using a 4-point parabolic fit to define time of occurrence of peaks.

JOINT II - Response at 4.6 m

<u>Event</u>	<u>1</u>	<u>2</u>	<u>3</u>	<u>Average</u>
u*	-27	+7	-15	-11
v**	-12	0	-20	-11
T°***	+18	+14	+3	+11

\* maximum offshore flow

\*\* in first event, correspond to maximum poleward; in the other, correspond to maximum equatorward.

\*\*\* minimum

JOINT II - Response at 80 m

<u>Event</u>	<u>1</u>	<u>2</u>	<u>3</u>
u*	0	+18	-12
v**	0	---	+24
T°***	---	---	---

\* maximum onshore

\*\* maximum poleward

\*\*\* minimum

--- it is not possible to recognize a peak value associated with the wind



much quantitative information is available. In event 1, the maximum of  $u$  and  $v$  have zero lag with the maximum wind. In the other two events there is no clear tendency, perhaps due to the scarcity of events.

#### F. Summary of Salient Features

Before proceeding with the dynamics of upwelling events, I review some of the salient features of the flow and temperature changes during events. Some of the patterns are common to Oregon and Peru, and others are contrasts between the two areas.

(1) Both components of the flow intensify during events, and there is a general cooling of the surface waters. At the surface, peak values reached by  $u$  and  $v$  are one standard deviation higher than the complete record mean.

(2) Off Oregon and Peru the trans-isobath flow during events is offshore at the surface (0-20 m approx.) and onshore at the interior. An offshore flow appears close to the bottom and is associated with the poleward undercurrent, suggesting the presence of a bottom Ekman layer.

(3) The surface offshore flow is strongly coupled with the wind. Small fluctuations in the wind stress are reflected in the  $u$  component but not in  $v$  or  $T$ .

(4) The thickness of the layer with onshore flow is larger than the thickness of the surface layer with offshore flow.

(5) The alongshore flow during events is equatorward in the surface, except off Peru where in event 1 all the water was flowing poleward.

There is a poleward undercurrent off both Oregon and Peru. In Oregon it disappears during events, and appears again during relaxation of the

events; usually three or four days after the maximum wind. On the contrary, off Peru, the undercurrent was present all the time.

(6) A short period of poleward wind off Oregon produces downwelling conditions: the surface flow is onshore, the equatorward flow is weak and the poleward undercurrent intensifies.

(7) The effect of strong wind stress during events is felt by  $u$  and  $v$  almost simultaneously and in all the water column. Even during the antievent off Oregon, the change is felt by the flow in all depths.

(8) Off Oregon the maximum offshore flow occurs simultaneously with the maximum wind, i.e., the lag is not significantly different from zero. Off Peru the maximum offshore flow tends to precede the maximum wind by a day or less. The surface equatorward flow reaches a maximum in a time that on the average is comparable to the inertial period (17 hours) off Oregon, and less or equal to a day off Peru (in all cases less than an inertial period which is 46 hrs.). Surface temperatures off Oregon takes a day or more to change and less than a day off Peru. In general, the values of time lags calculated here do not present a clear pattern, then no physical meaning could be associated with them. Nevertheless the response of the flow and temperature indicate that maxima are reached within one day of the maximum wind with a time lag of less than a day.

#### IV. DYNAMICAL ASPECTS OF UPWELLING EVENTS

##### A. Formulation of the Momentum Equations

One of the tools that physical oceanographers have available to analyze the dynamics of the ocean is the study of the balance between the different terms in the equations of motion (the momentum equations). The relative magnitude of the terms characterize the balances of forces in different places of the ocean. In this chapter I examine to what extent the relations between the terms of the momentum equations during events are similar to the mean momentum budgets during the upwelling season. Here I shall contrast, if only qualitatively, the average balances found in the literature (Smith, 1974; Allen and Kunda, 1978; Brink et al, 1978 and 1980) with what occurs during individual events.

A conventional cartesian coordinate system (x, y, z) will be used. Velocity components are u, v, and w. Then the continuity and momentum equations are:

$$\begin{aligned}\vec{\nabla} \cdot \vec{U} &= 0 \\ \vec{U}_t + 2\vec{\Omega} \times \vec{U} &= -\rho^{-1} \vec{\nabla} p + \nu \vec{\nabla}^2 \vec{U}\end{aligned}\tag{1}$$

A list of symbols and variables herein used is given in Appendix 1.

As is standard for the case of the ocean, I use linearized momentum equations in a rotating frame of reference (Pedlosky, 1979). The evaluation of nonlinear terms in (1) requires the introduction of alongshore derivatives. Here either I lack the necessary data or the spacing between sensors makes any estimation impractical. In addition, both Allen and Kundu (1978) and later Badan-Dangon (1980) presented

physical arguments that justified the neglecting of the non-linear terms in an upwelling area.

Now let us consider a uniform wind blowing over the sea surface:

$$\vec{\tau}(z,t) = i \tau^x(z,t) + j \tau^y(z,t)$$

then one can expand the linear momentum equations in the two horizontal components as:

$$u_t - fv = -\rho^{-1} p_x + \rho^{-1} \tau_z^x \quad (2)$$

$$v_t + fv = -\rho^{-1} p_y + \rho^{-1} \tau_z^y \quad (3)$$

To evaluate terms of equations (2) and (3) I used the velocity components obtained from current meters and the wind stress values. The terms that involve time derivatives were approximated applying a numerical central difference scheme with a time increment of 6 hrs.

For example to evaluate  $v_t$ :

$$v_t = (v(t + \Delta t) - v(t - \Delta t))/2\Delta t \quad (4)$$

Errors for this methodology are discussed by Allen and Kundu (1978).

The pressure term that involved x-derivatives was not calculated directly. However, Huyer (1980) showed that the dynamic height data, estimated from the density field, is probably a good representation of the sea surface along a section perpendicular to the coast. Changes in the sea level inferred from dynamic height data and extrapolated to the coast, agree well with changes of sea level right at the coast. These changes in sea level have an offshore scale of 30-60 km; the current meter mooring is 12 km from the coast. Thus, by using the sea level from tide gauges at the coast, and assuming that the sea level has a linear profile between the current meter arrays and the coast (i.e.,  $p_x$

constant), one can study if the currents are in geostrophic balance, i.e., one can compare the fluctuations in coastal sea level and in the alongshore current.

#### B. Review of the Mean Momentum Balance

In this section I examine some of the balances between terms in (2) and (3). A review of some of the most recent literature is also made. In addition, from information collected during CUE II and JOINT II, momentum balances were calculated, and are analyzed in the framework provided by the literature.

Very high correlation of  $v$  and the coastal sea level on the Oregon coast, support the assumption that the alongshore flow in the interior is in geostrophic balance (Smith, 1974; Allen, 1980). Furthermore, Allen and Kundu (1978) found that at 80 m off Oregon  $fv$  is substantially larger than  $u_t$ , suggesting that  $u_t$  is negligible in the x-momentum equation. Thus, (2) could be reduced to:

$$fv = \rho^{-1} p_x \quad (5)$$

Later I will compare  $fv$  and  $u_t$  during individual events, and see if the geostrophic balance for  $fv$  holds then. First I examine this relation for Oregon and Peru using the complete series of data. One sees that in both Oregon and Peru,  $fv$  is much greater than  $u_t$  (Fig. 12 and 13). Thus the assumption made in (5) is valid for both areas and at all three depths, i.e., a geostrophic balance between  $fv$  and the pressure term holds.

# OREGON

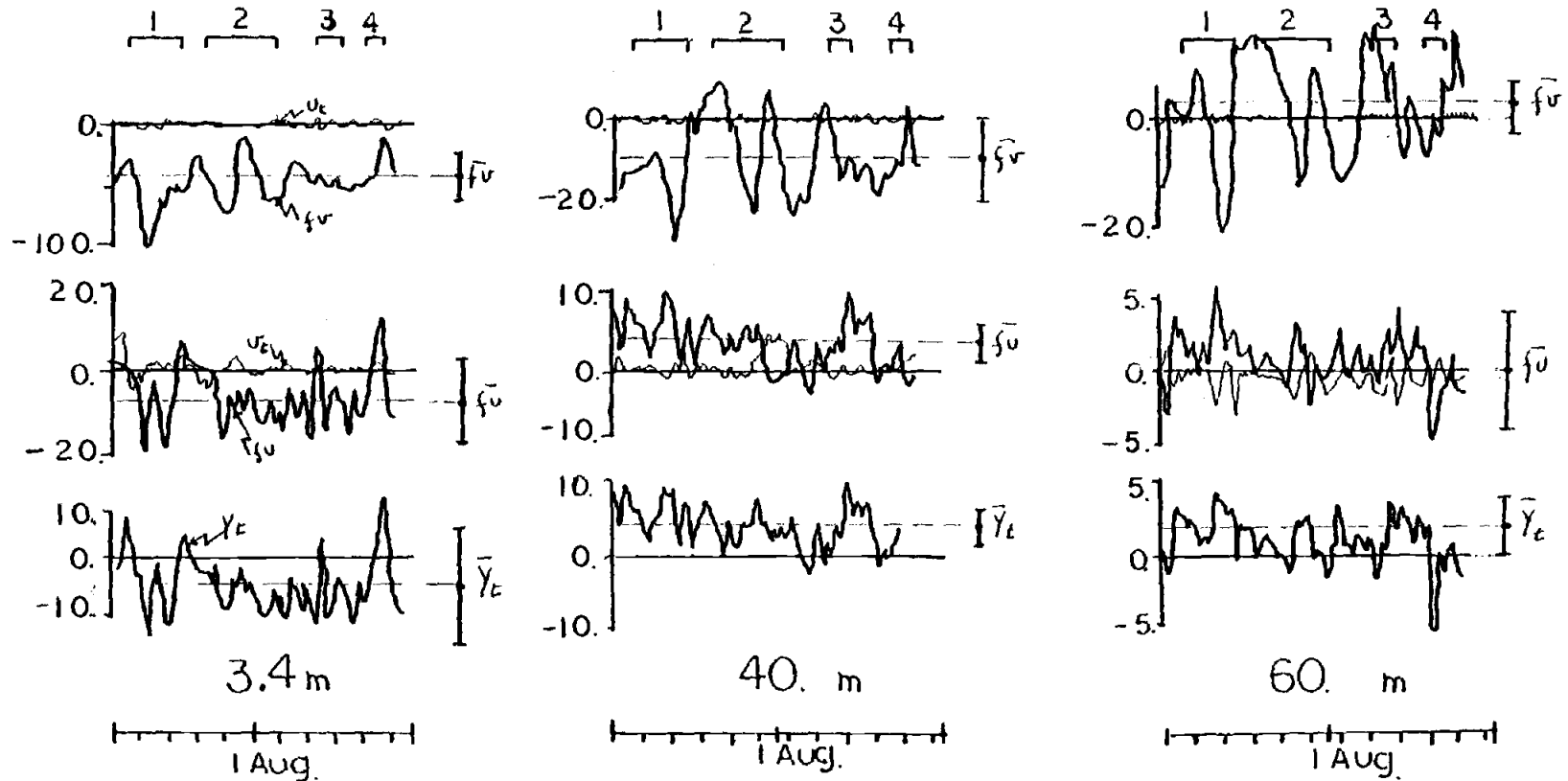


Figure 12 Time series of terms of the horizontal momentum equations at 3.4m, 40m, and 60m depth off Oregon. Mean and standard deviation are also shown. Units are  $10^{-4} \text{ cm s}^{-2}$ . Ticks on the time axes indicate 5 days periods.

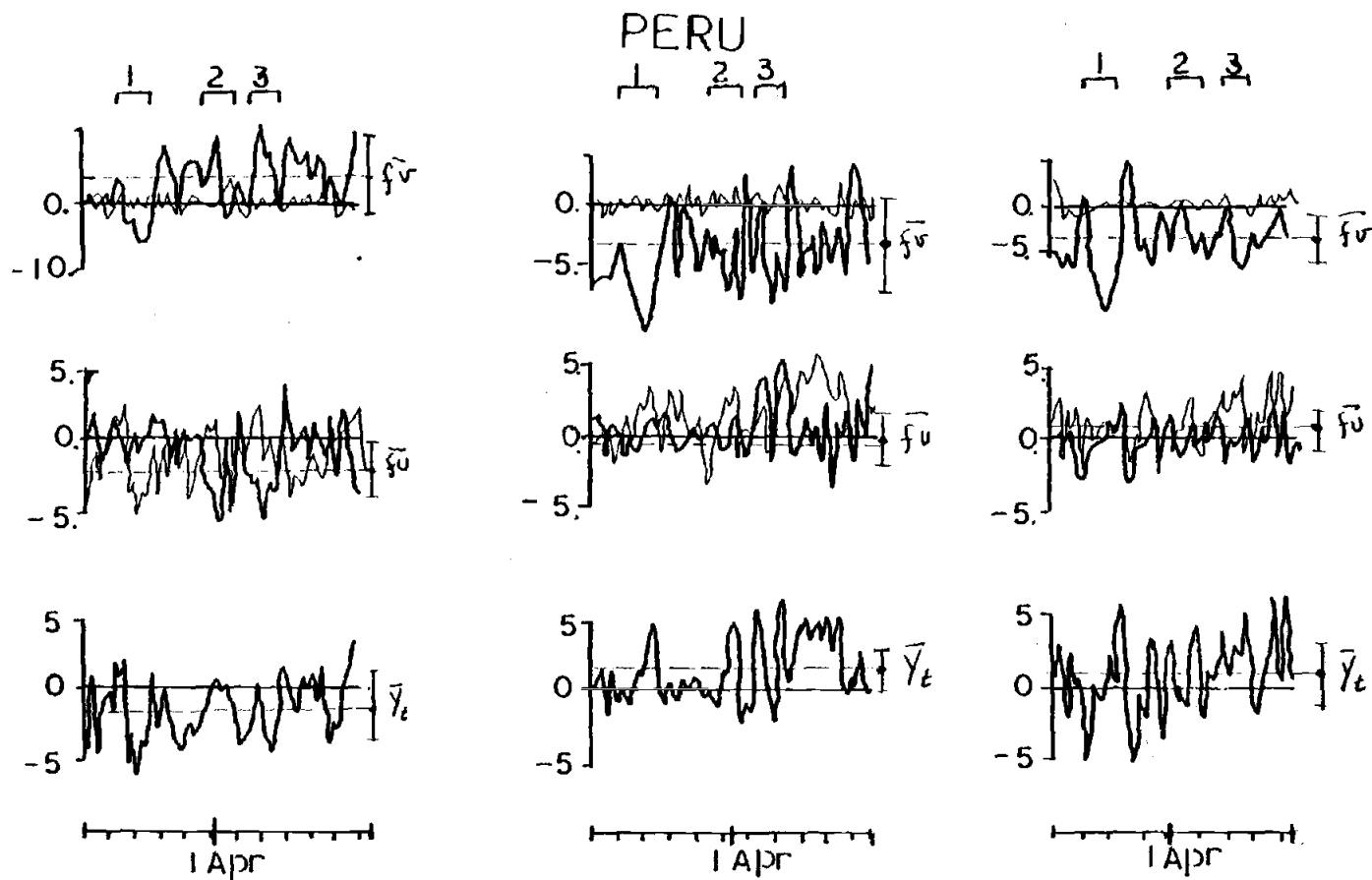


Figure 13 Time series of terms of the horizontal momentum equations at 4.6m, 39m, and 80m depth off Peru. Mean and standard deviation are also shown. Units are  $10^{-4} \text{ cm s}^{-2}$ . Ticks on the time axes indicate 5 days periods.

Since we are interested in upwelling, we also want to study the forcing problem. The most important forcing mechanism for upwelling is the alongshore component of the wind stress, which drives a cross-shelf transport in the surface Ekman layer. The expression for the transport in the surface layer due to the wind stress could be derived directly from (3), with the assumption that the coriolis term,  $f_u$ , balances the wind stress term. Integrating (3) over the surface frictional layer (D), gives the following expression for the transport in the surface layer:

$$\int_{-D}^0 u \, dz = \tau_w^y / (\rho f) \quad (6)$$

The Ekman transport ( $E_T$ ) is defined as  $\tau_w^y / \rho f$ . We define the measured offshore transport in the surface layer as  $T_S$ . If the volume balance is two dimensional, the offshore transport in the surface layer ( $T_S$ ) should be balanced by an onshore transport in the lower layer ( $T_L$ ).

Smith (1980) compared the observed transport  $T_S$  with  $E_T$ . For Oregon and Peru he found that the observed mean offshore transport is in fair agreement with the mean Ekman transport ( $E_T$ ). For Oregon  $E_T = -48 \cdot 10^2 \text{ cm}^3 / \text{cm sec}$  and  $T_S = -65 \cdot 10^2 \text{ cm}^3 / \text{cm sec}$ , which indicate that they are in fair agreement, but for Peru  $E_T = -141 \cdot 10^2 \text{ cm}^3 / \text{cm sec}$  and  $T_S = -82 \cdot 10^2 \text{ cm}^3 / \text{cm sec}$ , indicating that they are less comparable. On the other hand, the mean onshore transport in the interior was found to be larger than the offshore transport in the surface layer. (off Oregon  $T_L = 198 \cdot 10^2 \text{ cm}^3 / \text{cm sec}$  and off Peru  $T_L = 120 \cdot 10^2 \text{ cm}^3 / \text{cm sec}$ ). He concluded that upwelling is essentially three dimensional.



### C. Is the Alongshore Flow in Geostrophic Balance During Events?

In this section I investigate if the geostrophic assumption is valid during individual upwelling events. As in section IV-A, inferences of sea level fluctuations are made based on coastal tide gauge data.

Direct comparison of the sea level in Newport, Oregon and San Juan, Peru, with  $f_v$  at 40 m depth are used to test the geostrophic assumption during events. For comparison purposes the mean was removed from  $f_v$ , as was done for the sea level, thus the zero line corresponds to the mean values for both series (Fig. 14 a and b).

Changes in the Coriolis term  $f_v$ , off Oregon, are associated with the Newport sea level fluctuations (Fig. 14 a): a falling sea level at the coast is accompanied by an increase of the equatorward flow at the interior ( $f_v$  negative). Therefore, assuming that the coastal sea level is a good representation of  $P_x$ , the alongshore flow off Oregon is in geostrophic balance during events.

Off Peru, if the alongshore flow is in geostrophic balance, then an equatorward flow will be associated with a sea surface sloping down toward the coast. This type of relationship is inferred for event 1 from March 17th and on, and also during part of event 2 (Fig. 14b). However, in some other occasions the geostrophic relation during events off Peru was unclear, i.e., at the beginning of events 1 and 3. To study if other terms of (2) are important during events in Peru,  $u_t$  at 40 m depth was also plotted. But the results show that its contribution is negligible.

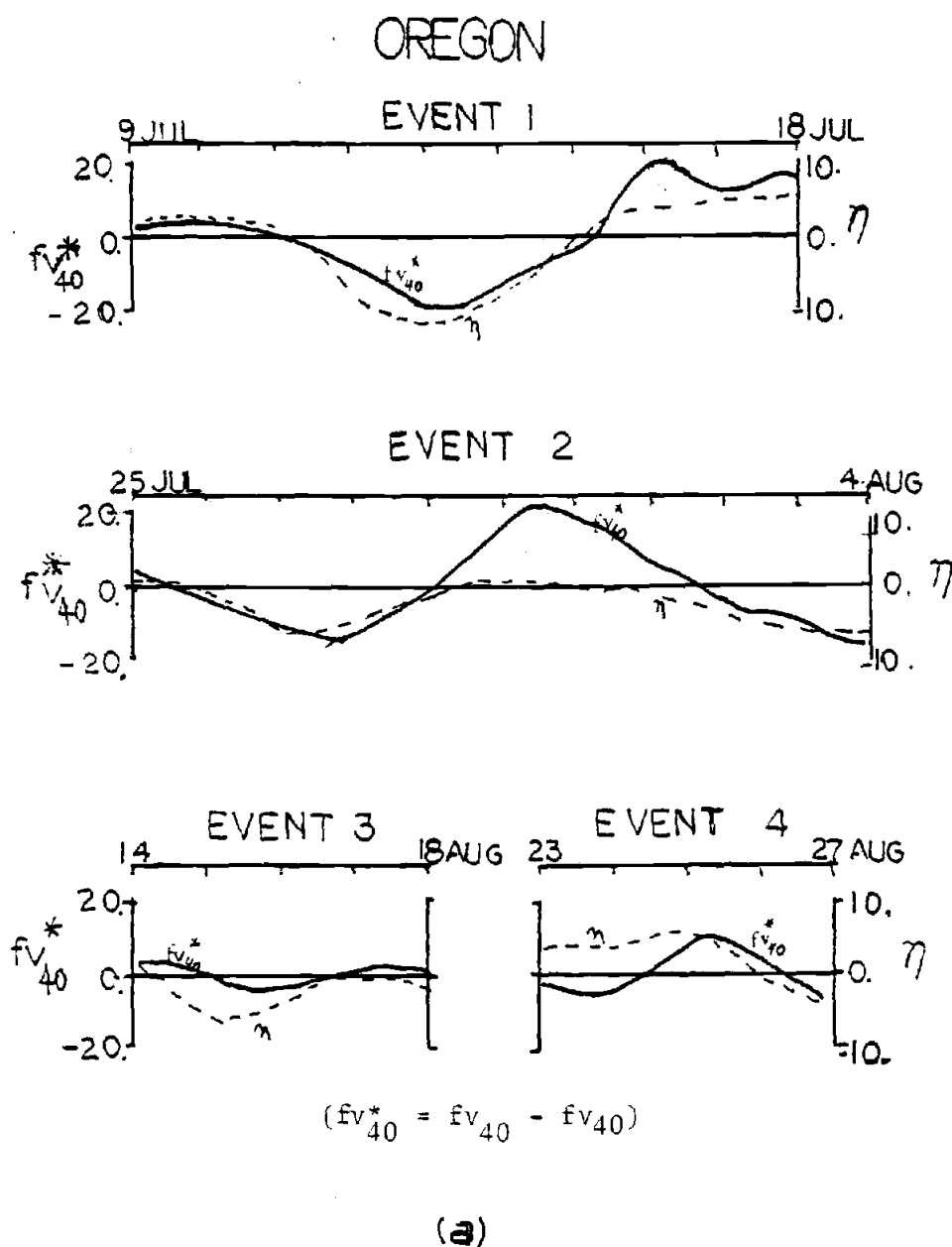


Figure 14 Cross-shelf momentum balance during events off:  
 (a) Oregon and (b) Peru. For calculations values at 40m were used (39m for Peru). Units are  $10^{-4}$   $\text{cm s}^{-2}$  for  $fv$ , and cm for the adjusted sea level at Newport (San Juan). The zero line correspond to the mean value for both time series.

## PERU

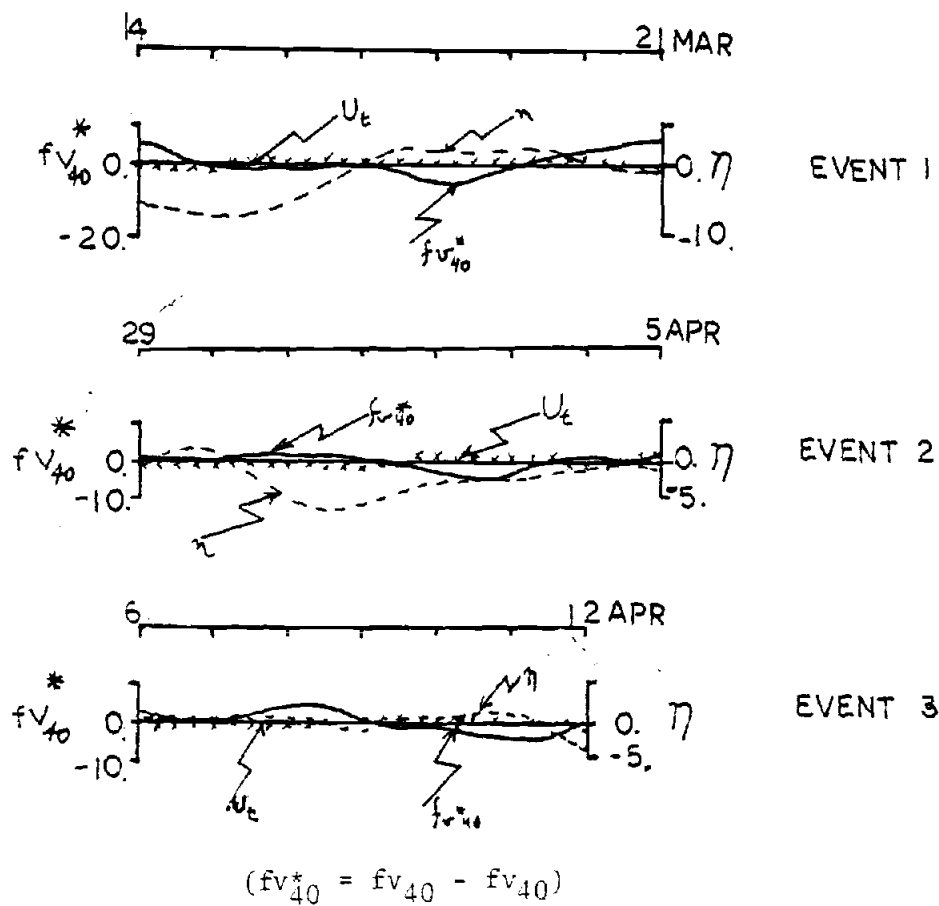


Figure 14b

#### D. Ekman Dynamics and Volume Budgets During Events

The basic assumption of the Ekman dynamics is that the Coriolis force,  $f_u$ , integrated over the surface layer balances the wind stress term in (3). The integration of these two terms over the surface frictional layer yields the characteristics expression for the Ekman transport, Eqs. 6.

There are some questions that can be addressed: Is the offshore transport in the surface layer ( $T_S$ ) in quantitative agreement with the Ekman transport ( $E_T$ ) computed directly from wind observations? Is the interior onshore transport larger than the surface offshore transport during events, as it is during the mean state? To find a quantitative answer to the questions, the volume transports during events were computed by trapezoidal integration of the "event mean" vertical profile of  $u$  components. For the calculations of the offshore transport during events (Table 2) the integration was made considering the contributions of all current meters located above a depth  $D$ . The depth  $D$  was taken to be the depth mid-way between the deepest current meter showing offshore flow and the next current meter below. The onshore transport was calculated by the integration of all the contributions of the current meters located below the depth  $D$ .

The mean Ekman transport computed from the average wind stress during each event ( $E_T$ ) and the measured mean transport in the upper ( $T_S$ ) and lower layers ( $T_L$ ) for events, are given in Table 5. The observed offshore transport during events is slightly larger than the computed Ekman transport. But the differences are the same order of magnitude as the overall mean values reported by Smith (1980). Thus, not much difference between the Ekman balance during events with that of the mean state are found here.

Table 5. Mean Ekman transport computed from the alongshore component of the wind stress during events ( $E_T$ ), measured cross-shelf transport in the surface ( $T_S$ ) and lower layers ( $T_L$ ) averaged during events. Transport is given in  $10^2 \text{cm}^3/\text{cm sec}$ , and is positive toward the coast.

<u>OREGON</u>	$E_T$	$T_S$	$T_L$
Event 1	-105	-132	+248
Event 2	- 80	-118	+176
Event 3	- 64	-116	+324
Average	- 83	-122	+249
<u>PERU</u>	$E_T$	$T_S$	$T_L$
Event 1	- 70	-109	+145
Event 2	- 68	-118	+ 89
Event 3	-108	-167	+344
Average	- 82	-131	+195

On the other hand, the onshore transport ( $T_L$ ) during events is larger than the offshore one. The large onshore transport ( $T_L$ ) in the lower layer of Oregon and off Peru may be a result of positive  $v_y$ , and not part of the compensatory flow for the surface offshore Ekman transport. A non-negligible mean  $v_y$  may be characteristic of coastal upwelling regions, as was pointed out by Smith (1980) and by Allen (1980).

#### E. Is the Cross-Isobath Flow in Geostrophic Balance with $p_y$ ?

The suggestion of Stommel and Leetmaa (1972) that the southwestward mean flow over the East coast of the United States requires a driving force other than the wind stress and density gradient, has been addressed later by Csanady (1976). The conclusion is that the extra driving force is an alongshore pressure gradient which produces a geostrophic onshore flow. An expression for that geostrophic flow could be derived from (3):

$$+fu = -\rho^{-1} p_y \quad (7)$$

The possibility of a geostrophic compensatory flow during events, was studied comparing curves of  $fu$  at 40 m depth with curves of  $p_y$  (Fig. 15 a and b). Off Oregon a sea level decreasing to the north would cause an onshore flow in the interior. Since the current meters are located between Garibaldi and Newport, the first attempt to search for a geostrophic balance was made between those two points (Fig. 15 a). But the association between curves of Ga - Ne and  $fu_{40}$  was poor and geostrophy is not even qualitatively suggested from this data. However, the pressure gradient calculated between Newport and Umpqua River have the correct sign to explain the positive  $fu$ , but not the magnitude

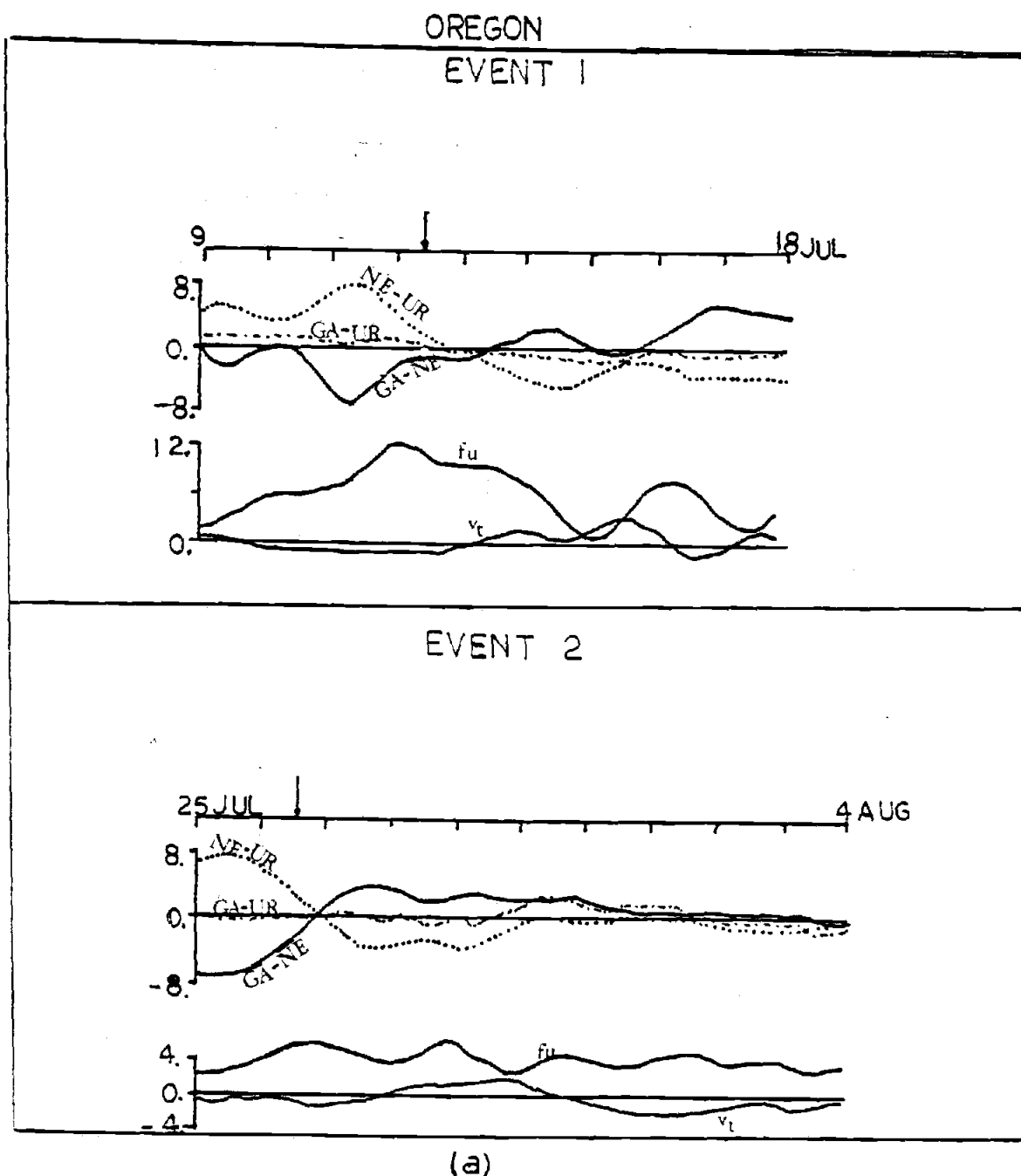
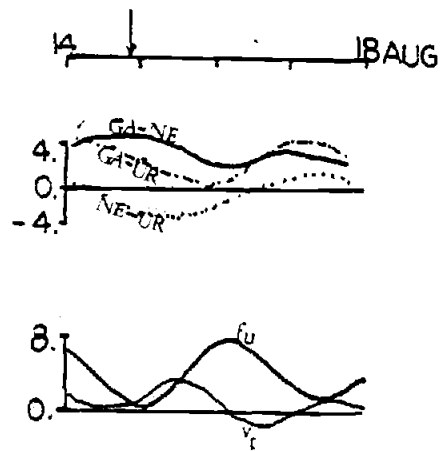


Figure 15 Momentum balance in the alongshore direction off (a) Oregon and (b) Peru. Values at 40m depth were used in calculations (39m for Peru). Units are  $10^{-4} \text{ cm s}^{-2}$ . The arrow on the time axis indicate the time of maximum wind stress. Pressure gradients off Oregon were calculated between Garibaldi (GA), Newport (NE), and Umpqua River (UR); off Peru were calculated between San Martin (SM) and San Juan (SJ).

OREGON  
EVENT 3

## EVENT 4

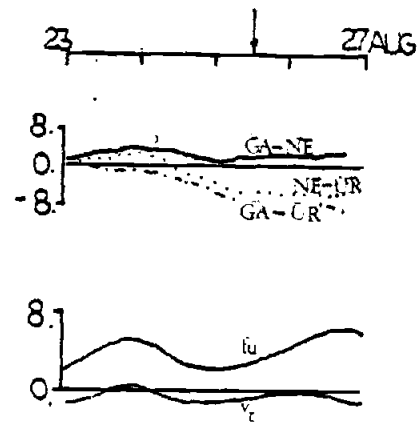


FIGURE 15 a (Continuation)



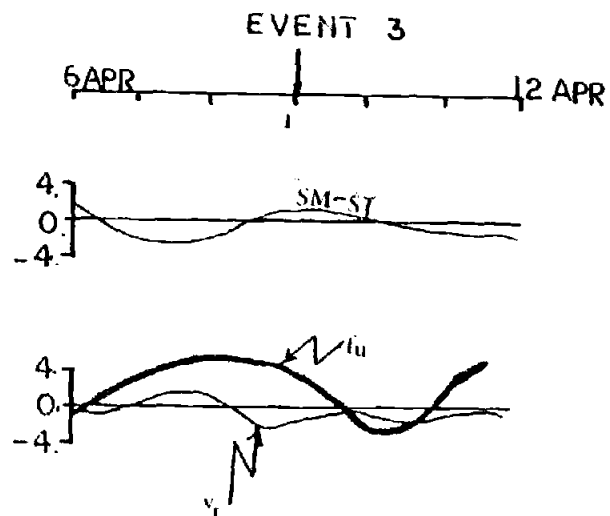
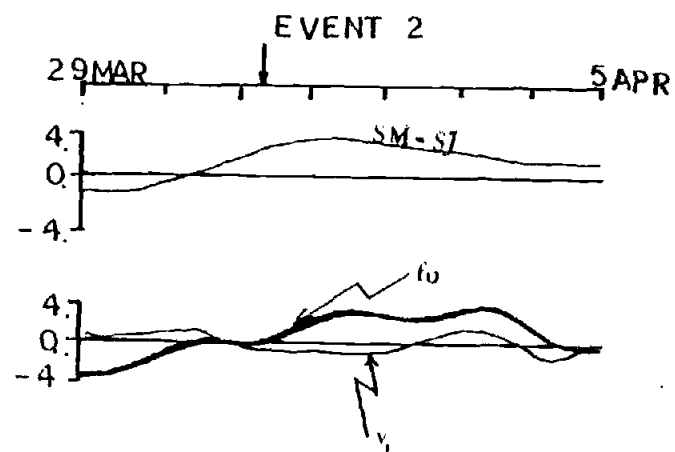
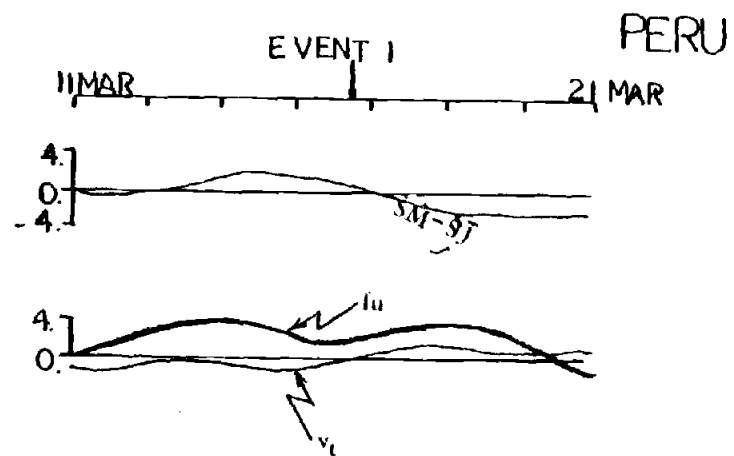


FIGURE 15 b

to balance the coriolis term. In addition, the poor correlation between the two curves (NE-UR and  $P_y$ ) indicate that the onshore flow is not in geostrophic balance off Oregon, during events.

Off Peru an onshore flow in the interior could be caused by a sea level sloping upward to the north (positive  $p_y$ ). The results of Fig. 15 show that most of the time there is no similarity between  $fu_{40}$  and  $P_y$ . Only during event 2 did a positive  $p_y$  correspond to a positive  $fu_{40}$  with both terms having similar magnitude.

#### F. Summary

Current, wind, and sea level data have been used to evaluate balances among terms of the equation of motion. Contrasts between the mean and the conditions during events have been made. The most salient features of this chapter can be summarized as:

- (1) The mean momentum balance is characterized off Oregon and Peru by:
  - An alongshore flow in geostrophic balance. The data presented here shows evidence of this relation over the continental shelf of Oregon and Peru.
  - A cross shelf momentum balance that is in good agreement with simple Ekman dynamics: The measured offshore transport agrees fairly well with the predicted from the computation of the Ekman transport.
  - Three dimensionality is important in the mean state. The onshore transport at the interior is larger than the offshore transport at the surface, indicating then that the mean upwelling is three dimensional.

- (2) A geostrophic alongshore flow was tested for individual events.

In both Oregon and Peru the alongshore flow is in geostrophic balance during events. However, transient departures from geostrophy were observed off Peru during some events.

- (3) Ekman dynamics and volume budgets were studied during selected events. The surface offshore transport and the calculated Ekman transport are in fair agreement. Differences in volume transport are of the same order of magnitude as the values for the mean state. As in the mean state, the interior onshore transport during events was almost twice the offshore transport at the surface. Three dimensional effects are important during events as well as during the mean state.

- (4) The possibility of a geostrophically balanced onshore flow in the interior during events was also studied. Comparisons of  $f u$  and  $p_y$  show that neither Oregon and Peru is there enough evidence to support such an assumption, at least during events.

## V. DISCUSSIONS AND CONCLUSIONS

### A. Response of the Flow and Temperature

It is widely known that upwelling occurs when an equatorward wind blows over the continental shelves of Oregon and Peru. However, one of the main motivations for this thesis was to ascertain whether or not a sudden increase of the wind above its mean would produce a response, that is significantly different from the already existing mean upwelling circulation, and, whether this response is dynamically analogous to that of the mean upwelling case.

Events occur on the shelf of Oregon (Halpern, 1976; Huyer, 1976), Northwest Africa (Huyer, 1976) and Peru (Brink et al, 1980) but, except for those papers, few quantitative studies of events have been made. The information presented here shows that both flow components and the temperature change markedly over the shelf in response to the upwelling favorable wind events. Fluctuations are one standard deviation larger than the overall record mean, in both Oregon and Peru. In addition, the effect of the wind event is felt by the cross shelf and alongshore components  $u$  and  $v$ , almost simultaneously throughout the water column, suggesting that the response is quasi-barotropic. In fact, Niiler (1975) suggested that the most energetic time-varying field over the shelf tend to be strongly barotropic.

The  $u$  component responds faster than  $v$  or  $T$ . Even small wind fluctuations are reflected on  $u$ . This is expected since  $v$  and  $T$  respond to cumulative effect of upwelling. An increase of  $v$  is related to the cumulative slope of the isopycnal in a section perpendicular to the coast (Allen, 1973), and a decrease of  $T$  is controlled by the temperature

of the incoming subsurface water mass, the surface heating and mixing (deSzoeke and Richman, 1981).

A dissipative mechanism for wind-driven time-dependent motion over the shelf is provided by turbulent friction (Allen, 1980; Csanady, 1981). During events when the equatorward flow is strong, the bottom friction opposes the wind stress and a bottom Ekman layer (BEL) develops. This frictional layer may increase the onshore flow near the bottom, by a physical process that is analogous to the frictional effect of the wind on the surface waters. However, the results (section III.D) show that during the peak of the wind the onshore flow near the bottom is less than at mid-depth. But when the wind relaxes and the poleward undercurrent appears, there is evidence of a bottom Ekman layer associated with the undercurrent but in this case the flow is offshore.

There is a strong equatorward flow at the surface, which, in most of the events, increases with the wind stress. Strong equatorward flow near the surface is characteristic of the upwelling of Oregon (Allen, 1973; Smith, 1974). Off Peru there is also a surface equatorward flow (Brink et al, 1980). However off Peru the surface current was not always equatorward in spite of persistent equatorward wind; i.e., during event 1 the flow near the surface was poleward, opposite to the wind. This fact contrasts with the other coastal upwelling regions. Off Peru the alongshore velocity field is not strongly driven by the local alongshore component of the wind stress. An explanation to the low correlation between alongshore current and local wind off Peru is related to the presence of baroclinic Kelvin waves, originated equatorwards of  $10^{\circ}\text{S}$  (Brink et al, 1978; Smith, 1978).

During events the poleward undercurrent was not present, except during the first event off Peru. However, it appears when the wind is relaxing (Mooers and Allen, 1973). The delay of three to four days after the maximum wind could be attributable to the generation of continental shelf waves suggested by Sugimotohara (1974). The same author, after theoretical considerations, indicates that after the forcing (wind stress) is stopped, the shelf waves propagate away from the upwelling region and the poleward undercurrent fully develops.

#### B. Time Scale of Events

For a long time the general thought was that the upwelling begins relatively long after the onset of the favorable wind. Yoshida (1955) suggested that "upwelling will be favored in the case when northerly winds parallel to the coast prevail for longer than a week over the waters". Quantitative studies of upwelling events indicated that the period between the onset of the wind and the maximum onshore transport is of the order of one to three days (Halpern, 1976). Another estimation on the coast of Oregon and Africa indicates that the response occurs in less than a day (Huyer, 1976). Quantitative estimations of the time lags between the maximum wind and the peak values of the flow and temperature were made here. Although a clear pattern was not found, the time response of the flow and temperature indicate that extremes are reached within less than a day of the peak wind stress. Indeed, indications were found that the maximum flow preceded the maximum wind. This situation has been previously reported by Mooers and Allen (1973).

Three explanations may be given: The upwelling is occurring shoreward of our point of observation, then the signal presented here could correspond to an advection of momentum from the coast where we do not know the time of the peak in the wind. Also, one has to consider that the filtering process could affect the wind and the current data in a different way, since their power spectra are also different (R.L. Smith, personal communication). And finally, shelf waves that arrive at the point of observation before the perturbation of the wind could be the cause of  $v$  preceding the wind stress.

### C. Momentum and Volume Balances

During events there is not much difference between the calculated Ekman transport and the measured offshore transport; this result agrees well with what is reported by Halpern (1976) and Smith (1980). On the other hand, the onshore flow was almost twice as large as the near surface westward flow, suggesting that the volume balance is three dimensional during events (dependent upon alongshore variations). This finding contrasts with Halpern (1976) and Huyer (1976) who reported that the mass balance was nearly two-dimensional during events.

An additional argument supporting the conclusion that events are three-dimensional is that if a linear two-dimensional balance exists, there will be a balance between  $v_t$  and  $fu$ . The occurrence of this type of balance would be indicated by small values of  $Y_t$  (Fig. 12 and 13). The results presented here indicate that there is no obvious relation between the variation of the wind stress and  $Y_t$  either off Oregon or

off Peru (Fig. 12 and 13). Thus there is no evidence for a tendency toward a two dimensional dynamic balance during periods of upwelling events. The same result was found at 80 m depth off Oregon by Allen and Kundu (1978) using a time series of  $V_t$  calculated with the same data as here. Brink et al (1980) suggests that the reasons for three dimensionality may be a combination of non-uniformities in the bottom topography and in the alongshore wind, which both have strong variations on the alongshore direction.

Tests at different depths indicate that the equatorward flow is in geostrophic balance during events. This conclusion has been shown, using the same assumption as in Chapter IV, for the complete series of data by Allen and Kundu (1978), Brink et al (1980).

The possibility that longshore pressure gradient could support a geostrophic exchange of mid-ocean water with the shelf (Niiler, 1975; Csanady, 1976) was tested for events. Results show no evidence of such geostrophic onshore flow. In addition Brink et al (1980), tested the mean balance between  $v_t$ ,  $P_y$ , and  $fu$ ; the poorest balance was between the Coriolis term and the pressure gradient. Therefore there is no evidence of an onshore geostrophic flow in the mean or in the event time scale.

In this thesis the physical characteristics of upwelling events off Oregon and Peru were described. The criteria used to select the events and the availability of data, limited the number of events selected; and so the representativeness of the data. Longer time series of current measurement, in both locations, could contribute with valuable



information. In spite of the scarcity of data presented here, differences were found between the two locations. Off Peru the forcing of the wind is not so clear as off Oregon. In the literature, this fact is related to low-frequency (subtidal) fluctuations that propagate poleward, apparently from an equatorial or near-equatorial source (Huyer, 1980). Experiments to compare the California current system with the Peru-Chile current system, and specially to study the generation and propagation of low frequency fluctuations off the West coast of South America should be made.

#### D. Conclusions

1. Periods of strong equatorward winds off Oregon and Peru, called upwelling events, produce a clear response of the coastal waters. During upwelling events, both temperature and horizontal flow intensify; the peak values reached by them, at the surface, are greater than the mean by one standard deviation.
2. Calculations of time lag indicate that the offshore flow off Oregon is closely coupled to the wind and fluctuates with a zero lag. Off Peru precede the wind by a half a day. The alongshore flow, at the surface, lags the wind by less than a day.
3. Off Oregon a poleward undercurrent appears when the wind is relaxing. This occurs in approximately three to four days after the maximum wind. Off Peru the poleward undercurrent is present all the time, however it weakens during events; except during event 1 in which it increases significantly throughout the water column.

4. The dynamics of an upwelling event is fairly similar to the mean momentum balance in an upwelling zone: the alongshore flow is in geostrophic balance, and the Ekman transport calculated from wind data agrees with the surface offshore transport measured by the current meters. The interior onshore transport is at least twice the offshore transport at the surface, suggesting that three dimensionality is important during events as well as during the mean upwelling.

## BIBLIOGRAPHY

- Allen, J. S. 1973. Upwelling and coastal jets in a continuously stratified fluid. *J. Phys. Oceanogr.*, 3, 245-257.
- Allen, J. S. 1980. Models of wind-driven currents on the continental shelf. *Ann. Rev. Fluid Mech.*, 12, 389-433.
- Allen, J. S. and P. K. Kundu. 1978. On the momentum, vorticity and mass balance off the Oregon coast, *J. Phys. Oceanogr.*, 8, 13-27.
- Allen, J. S., and R. D. Romea. 1980. On coastal-trapped waves at low latitudes in a stratified ocean. *J. Fluid Mech.*, 98, 555-585.
- Badan-Dangon, A. 1980. On the dynamics of subinertial currents off northwest Africa. Ph.D. Dissertation, Oregon State University, Corvallis, Oregon, 130 pp.
- Brink, K. H., J. S. Allen and R. L. Smith. 1978. A study of low-frequency fluctuations near the Peru coast. *J. Phys. Oceanogr.*, 8, 1025-1041.
- Brink, K. H., D. Halpern and R. L. Smith. 1980. Circulation in the Peruvian upwellings system near 15°S. *J. Geophys. Res.*, 85, 4036-4048.
- Csanady, G. T. 1976. Mean circulation in shallow seas. *J. Geophys. Res.*, 81, 5389-5399.
- Cutchin, D. L. and R. L. Smith. 1973. Continental shelf waves: low frequency variations in sea level and currents over the Oregon continental shelf. *J. Phys. Oceanogr.*, 3, 73-82.
- deSzoeko, R. A., and J. G. Richman. 1981. The role of wind-generated mixing in coastal upwelling. Submitted to *J. Phys. Oceanogr.*
- Ekman, V. M. 1905. On the influence of the earth's rotation on ocean currents, *Arkiv. Mat. Astron. Fysik*, 12, 1-52.
- Enfield, D. B., R. L. Smith, and A. Huyer. 1978. A compilation of observations from moored current meters, vol. 13, wind currents and temperature over the continental shelf and slope off Peru during JOINT II. Oregon State University, School of Oceanography, Data Rep. 70, Ref. 78-4, 343 pp.
- Halpern, D. 1976. Structure of a coastal upwelling event observed off Oregon during July 1973. *Deep-Sea Res.*, 23, 495-508.

- Halpern, D., J. R. Holbrook, and R. M. Reynolds. 1974. A compilation of wind current and temperature measurements, Oregon. July and August, 1973. CUEA Tech. Rep. 6, Ref. 74-23, Dept. of Oceanography, University of Washington, Seattle, Washington, 190 pp.
- Huyer, A. 1976. A comparison of upwelling events in two locations: Oregon and Northwest Africa. *J. Mon. Res.*, 34, 531-546.
- Huyer, A. 1980. The offshore structure and subsurface extension of sea level variations off Peru, 1976-1977. *J. Phys. Oceanogr.*, 4, 1755-1768.
- Huyer, A., Smith, R. L. 1978. Physical characteristics of Pacific Northwestern coastal waters. *In the Marine Plant Biomass of the Pacific Northwest Coast*, ed. R. Krauss, 37-55. Corvallis: Oregon State Univ. Press.
- Krauss, E. B. 1972. *Atmosphere Ocean Interaction*. Oxford University Press, 275 pp.
- Mooers, C. N. K. 1976. Wind-driven currents on the continental margin. *Marine Sediment Transport and Environmental Management*. D. J. Stanley and D.J.P. Swift, eds., John Wiley & Sons, New York, 29-46.
- Mooers, C. N. K. and R. L. Smith. 1968. Continental shelf waves off Oregon. *J. Geophys. Res.*, 73, 549-557.
- Mooers, C. N. K., J. S. Allen. 1973. Final report of the Coastal Upwelling Ecosystems Analysis. Summer 1973 Theoretical Workshop. School of Oceanography, Oregon State University, Corvallis, Oregon.
- Niiler, P. P. 1975. A report on the continental shelf circulation and coastal upwelling, *Reviews of geophysics and space physics*, 13(3), 609-614.
- Pedlosky, J. 1979. *Geophysical Fluid Dynamics*. Springer-Verlag, New York Inc., 624 pp.
- Pillsbury, R. D., J. S. Bottero, R. D. Still and W. E. Gilbert. 1974. A compilation of observations from moored current meters. Vol. VII: Oregon Continental Shelf, July-August 1973. Data Rep. 21, Ref. 74-7, Oregon State University, Dept. of Oceanography, Corvallis, Oregon, 87 pp.
- Smith, R. L. 1974. A description of current, wind and sea level variations during coastal upwelling off the Oregon coast, *J. Geophys. Res.*, 79, 435-443.
- Smith, R. L. 1978. Poleward propagating perturbations in currents and sea levels along the Peru coast. *J. Geophys. Res.*, 83, 6083-6092.

- Smith, R. L. 1980. A comparison of the structure and variability of the flow field in the three coastal upwelling regions: Oregon, Northwest Africa, and Peru. IDOE International Symposium on Coastal Upwelling, Los Angeles, 4 February 1980.
- Stommel, H., and A. Leetmaa. 1972. The circulation on the continental shelf, Proc. Nat. Acad. Sci., USA, 69, 3380-3384.
- Suginohara, N. 1974. Onset of coastal upwellings in a two-layer ocean by wind stress with longshore variations. J. Oceanogr. Soc. JPM, 30, 23-33.
- Winant, C. D. 1980. Downwelling over the southern California shelf. J. Phys. Oceanogr., 10(5), 721-799.
- Yoshida, K. 1955. Coastal upwelling off the California coast. Rec. Oceanogr. Wks. Jep., 2(2), 8-20.
- Yoshida, K. 1967. Circulation in the eastern tropical oceans with special references to upwelling and undercurrents. Jap. J. Geophyscs. 4(2), 4-75.

## APPENDIX I

1. Notation

$C_d$	drag coefficient
$E_T$	Ekman transport in the surface layer
$f$	Coriolis parameter
$f_v, f_u$	Coriolis term in the momentum equations
$H$	water depth
$\bar{N}$	vertical averaged Brunt-Vaisala frequency (a measure of stratification)
$\Omega$	earth's angular valocity ( $7.3 \cdot 10^{-5} \text{ s}^{-1}$ ).
$P$	Hydrostatis pressure
$P_x, P_y$	spacial derivative of the pressure term in x and y directions
$R$	baroclinic Rossby radius of deformation
$\rho_A$	air density
$\rho$	water density
$T_S$	offshore transport in the surface layer
$T_L$	onshore transport in the interior layer
$\tau^x, \tau^y$	component of the wind stress in the x and the y direction, respectively.
$u, v, w$	velocity components; positive values are, u-eastward, v-northward, and w-upward.
$U_w, V_w$	components of the wind velocity in the x and y directions, respectively
$u_t, v_t$	time derivatives of the u and v velocity components
$x, y, z$	right-handed Cartesian coordinate system
$\eta$	sea level
$\Delta t$	time increment
$\nu$	coefficient of turbulent viscosity